Adaptive Chip-Rate Equalization of Downlink Multirate Wideband CDMA

A Thesis

Presented in Partial Fulfillment of the Requirements for

the Degree Master of Science in the

Graduate School of The Ohio State University

By

Adam R. Margetts, B.S. Electrical Engineering and Mathematics

* * * * *

The Ohio State University

2002

Master's Examination Committee:

Philip Schniter, Adviser

Hesham El Gamal

Approved by

Adviser

Department Electrical Engineering

© Copyright by

Adam R. Margetts

2002

ABSTRACT

We consider a downlink DS-CDMA system in which multirate user signals are transmitted via synchronous orthogonal short codes overlaid with a common scrambling sequence. The transmitted signal is subjected to significant time- and frequency-selective multipath fading, e.g., a channel with delay spread potentially longer than the bit interval of high-rate users.

In response to this scenario, a novel two-step receiver is proposed that combines chip-rate adaptive equalization with error filtering. In the first step, a code-multiplexed pilot is used to adapt the equalizer. Single-pole averaging of the chip-rate error signal used in adaptation reduces MAI and implies third-order LMS, which has advantages over standard LMS in tracking the time-varying channel. In the second step, decision-direction is used to improve the error signal, resulting in improved tracking performance. The performance of the adaptive receiver is studied through analysis and simulation.

Adaptive Chip-Rate Equalization of Downlink Multirate Wideband CDMA

By

Adam R. Margetts, M.S.

The Ohio State University, 2002

Philip Schniter, Adviser

We consider a downlink DS-CDMA system in which multirate user signals are transmitted via synchronous orthogonal short codes overlaid with a common scrambling sequence. The transmitted signal is subjected to significant time- and frequency-selective multipath fading, e.g., a channel with delay spread potentially longer than the bit interval of high-rate users.

In response to this scenario, a novel two-step receiver is proposed that combines chip-rate adaptive equalization with error filtering. In the first step, a code-multiplexed pilot is used to adapt the equalizer. Single-pole averaging of the chip-rate error signal used in adaptation reduces MAI and implies third-order LMS, which has advantages over standard LMS in tracking the time-varying channel. In the second step, decision-direction is used to improve the error signal, resulting in improved tracking performance. The performance of the adaptive receiver is studied through analysis and simulation.

Dedicated to Ruth Ann

ACKNOWLEDGMENTS

My wife Ruth lent me mental, physical, and spiritual support throughout my time at Ohio State. I am indebted to her for the sacrifices she made to help me succeed.

Dr. Philip Schniter–MS advisor, idea-generator, and taskmaster–deserves many many thanks for his patience and help in completing this thesis, and for all the enjoyable ultimate frisbee games. I thank Dr. Hesham El Gamal for being a part of my thesis committee and imparting knowledge of communication system fundamentals. His favorite question was "what are the basic principles here?"

My work experience at Thomson Multimedia was the impetus for this thesis. Special thanks to the physical layer group: Kumar Ramaswamy, Louis Litwin, Alton Keel, Paul Knutson, Wen Gao, and Zoran Kostic.

Special thanks to my friends in the lab. Brian, Siddharth, Bijoy, Ravi, Dephne, Emre, and Jing were a source of intellectual stimulation and entertainment. Deep and diverse were the conversations with Brian, and Siddharth lightened the atmosphere with his accurate impersonations of all our favorite professors. Bijoy and Ravi were the brains of the outfit, Dephne was the hard worker, Emre was the quiet one, and Jing provided unparalleled technical support. I wish also to thank the many friends in our church congregation, who made us feel welcome in our new home.

VITA

April, 1975	Born - Bountiful, Utah
May, 2000	B.S. Electrical Engineering and Mathematics, Utah State University
2000-2001	Dayton Area Graduate Studies Institute Fellow
2002-	Ohio Space Grant Consortium Fellow

PUBLICATIONS

Conference Publications

P. Schniter and A. Margetts, "Adaptive Chip-Rate Equalization of Downlink Multirate Wideband CDMA". *Proc. Asilomar Conf. on Signals, Systems, and Computers*, (Pacific Grove, CA), Nov 2002.

Patents

L. Litwin, A. Margetts, and P. Knutson, "Multi-Stage Automatic Gain Control For Spread-Spectrum Receivers". *U.S.P.T.O. Patent Pending*, filed July 2002

A. Margetts and L. Litwin, "Synchronization Strategy and Architecture for Spread-Spectrum Receivers". *U.S.P.T.O. Patent Pending*, filed July 2002

FIELDS OF STUDY

Major Field: Electrical Engineering

Studies in:

Detection and Estimation Theory, Signal Processing	Prof. Philip Schniter
Communication Theory	Prof. Hesham El Gamal

TABLE OF CONTENTS

Page

LIST OF TABLES

Table **Page**

LIST OF FIGURES

CHAPTER 1

INTRODUCTION

1.1 Motivation

Wireless communication has grown phenomenally in the last few years. Demand for higher-bandwidth mobile applications is fuelling the current interest in developing new cellular systems. In third generation (3G) cellular systems, data rates in the downlink (from base to mobile) are expected to be greater than in the uplink. In other words, system designers are expecting people to use applications that consume data faster than they produce data. Applications that fit this model include internet browsing, downloading email with picture content, and viewing streaming video. Traffic can be bursty or continuous. Due to the myriad of applications, their sundry bandwidth and quality of service requirements, and the harsh mobile channel conditions, direct sequence code division multiple access (DS-CDMA) has become the physical-layer waveform of choice for 3G systems. Since this thesis studies the DS-CDMA downlink, we assume a synchronous DS-CDMA system throughout (we also shorten DS-CDMA to CDMA).

CDMA used in 3G systems solves the non-symmetric user-bandwidth problem by allocating shorter spreading codes to higher-rate users, and longer spreading codes

to lower-rate users, while keeping the chip rate constant. Hence, the transmitted bandwidth is constant regardless of the bit-rate. Codes are chosen from an orthogonal code-space defined by a Hadamard matrix so that all active codes are orthogonal. Each user is assigned a code, and each bit is mapped onto the code. The downlink code streams are summed to create a synchronous, aggregate, multi-user chip-rate signal.

An assumption that makes this thesis different from much of the CDMA literature is that a scrambling code sequence is applied to the transmitted chip-rate signal. In 3G systems the base-station specific scrambling code separates cells to facilitate dense frequency re-use. Inter-cell interference appears as background noise, and the orthogonal codes may be re-used in neighboring cells (in the same frequency band). However, the scrambling code destroys signal cyclo-stationarity, upon which usual methods for multipath and multi-access interference (MAI) mitigation in CDMA are based [2][3].

As previously suggested, the downlink traffic may be bursty or continuous. Because data can be received continuously, a perpetual pilot signal is multiplexed into the transmitted chip-stream. Though block fading models are inappropriate, in some derivations we assume that the channel is fixed, which is approximately true over short time intervals.

The multiuser signal passes through a frequency- and time-selective channel en route to the mobile receiver. Frequency-selective fading arises when channel memory, due to echoes, causes past chips to interfere with present chips. Channel memory occurs in rich scattering environments, e.g., urban environments. Frequency selectivity destroys the orthogonality between user codes, which introduces MAI into bit

estimates from the matched filter receiver. The matched filter receiver, standard in CDMA systems, is known to suffer from MAI [4]. Time-selectivity is introduced when there is relative motion between the base station and the mobile, or when objects in the vicinity are moving. The rate of channel variation is directly proportional to the relative velocity and to the carrier frequency. It is paramount for receivers to adapt to changing channel conditions as quickly as possible, preferably at chip-rate.

The goal of this thesis is to design algorithms to adaptively equalize the chip-rate frequency- and time-selective channel. By doing this the orthogonality of the multiuser signal is restored and MAI can be removed by despreading. In conflict with the greater demand on downlink performance is the requirement that mobile units consume little power, thus algorithms must be computationally feasible.

1.2 Organization & Contributions

In this thesis we present adaptive solutions to equalize the received signal of a CDMA downlink where scrambling has been applied to the transmitted signal. The transmitted signal is subjected to frequency- and time-selective Rayleigh fading and AWGN noise. We derive the optimal MMSE equalizer and give the signal to interference plus noise ratio (SINR) expression.

1.2.1 Adaptive Equalizers

A novel averaged-error LMS algorithm is derived and shown to converge in the mean to the optimal MMSE solution, and is shown to have superior tracking qualities over the standard LMS algorithm. The averaged-error LMS algorithm is trained with a continuous pilot channel, and updates come at chip rate.

A chip-level decision-directed (DD) equalizer is suggested and shown, through simulation, to approach the optimal performance of the theoretical MMSE equalizer in frequency-selective time-varying channels. The DD algorithm is adapted with the delayed received signal due to inherent delays in making symbol estimates in a CDMA system, e.g., for a bit-stream with longest spreading factor N_0, we must wait N_0 chips before making symbol decisions and re-spreading and scrambling. The DD algorithm is shown to be robust to bit errors due to the presence of the pilot signal.

CHAPTER 2

BACKGROUND

2.1 Multirate CDMA

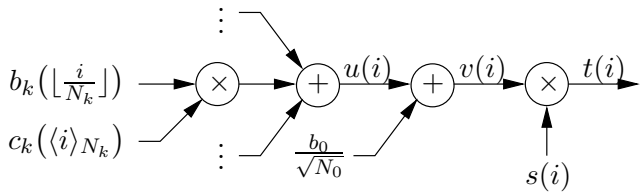

Figure 2.1: Synchronous Downlink Chip-Spaced Model

Variable	Definition
K	number of users
N_k	k^{th} user's spreading gain
$b_k(n)$	k^{th} user's bit stream
$c_k(i)$	k^{th} user's short code
$u(i)$	multiuser sequence
$s(i)$	scrambling sequence
$v(i)$	multiuser sequence plus pilot
$t(i)$ or t_i	transmitted sequence

Table 2.1: Variable definitions for transmitted multirate CDMA signal

We make the following assumptions about the transmitter:

A.1) *Circular, i.i.d., zero-mean, PSK scrambling*:

$$\forall i,\ |s(i)| = 1; \quad \mathrm{E}\{s(i)s^*(i+j)\} = \delta_j.$$

A.2) *Multirate orthonormal Walsh codes*:

$$\forall k,\ \ell \text{ s.t. } N_\ell \geq N_k,\ m \in \{0, \ldots, \tfrac{N_\ell}{N_k} - 1\}, j :$$
$$\delta_{\ell-k} = \sum_{i=0}^{N_k-1} c_k^*(i) c_\ell(i+mN_k), \quad |c_k(j)| = \frac{1}{\sqrt{N_k}}$$

As an example, we might start with the $N = 4$ Walsh codes and combine the latter two codes into a rate-2 code that is orthonormal in the sense above:

$$\frac{1}{2}\begin{Bmatrix} 1 & 1 & 1 & 1 \\ 1 & 1 & -1 & -1 \\ 1 & -1 & -1 & 1 \\ 1 & -1 & 1 & -1 \end{Bmatrix} \rightarrow \frac{1}{2}\begin{Bmatrix} 1 & 1 & 0 & \sqrt{2} \\ 1 & 1 & 0 & -\sqrt{2} \\ 1 & -1 & \sqrt{2} & 0 \\ 1 & -1 & -\sqrt{2} & 0 \end{Bmatrix} \rightarrow \frac{1}{2}\begin{Bmatrix} 1 & 1 & \sqrt{2} \\ 1 & 1 & -\sqrt{2} \\ 1 & -1 & 0 \\ 1 & -1 & 0 \end{Bmatrix}$$

A.3) *Constant pilot at "user" index $k=0$*:

$$\forall n,\ b_0(n) = b_0; \quad c_0(i) = \begin{cases} \frac{1}{\sqrt{N_0}} & 0 \leq i \leq N_0 - 1 \\ 0 & \text{else} \end{cases}$$

A.4) *Circular, independent, zero-mean user bits ($k > 0$)*:

$$\forall n, m, k \neq 0,\ \mathrm{E}\{b_k(n) b_\ell^*(n+m)\} = P_k \delta_m \delta_{\ell-k}.$$

where P_k is the symbol power of the k^{th} user.

A.5) *Zero-mean, circular, white, Gaussian noise w_m with variance σ_w^2.*

From Fig. 2.1 we write the transmitted signal as

$$t(i) = v(i)s(i) \tag{2.1}$$

which from A.1)-A.4) is zero-mean uncorrelated with power

$$\sigma_t^2 \ = \ \mathrm{E}\,|v(i)|^2\,\mathrm{E}\,|s(i)|^2 \ = \ \mathrm{E}\left|\frac{b_0}{\sqrt{N_0}} + u(i)\right|^2 \mathrm{E}\,|s(i)|^2 \ = \ \frac{|b_0|^2}{N_0} + \sigma_u^2 \tag{2.2}$$

where

$$v(i) \;:=\; \frac{b_0}{\sqrt{N_0}} + u(i) \tag{2.3}$$

$$u(i) \;:=\; \sum_{k=1}^{K} c_k\big(\langle i \rangle_{N_k}\big) b_k\big(\lfloor \tfrac{i}{N_k} \rfloor\big) \tag{2.4}$$

and

$$\sigma_u^2 \;=\; \sum_{k=1}^{K} \big|c_k\big(\langle j \rangle_{N_k}\big)\big|^2 \,\mathrm{E}\big[\big|b_k\big(\lfloor \tfrac{j}{N_k} \rfloor\big)\big|^2\big] \;=\; \sum_{k=1}^{K} \frac{P_k}{N_k}$$

Note that $\sigma_v^2 = \sigma_t^2$.

2.2 Fading Channel Model

In this thesis we make the standard wide-sense stationary uncorrelated-scattering Rayleigh-fading channel model assumptions [5]. In the following, the channel h_m is the combined response of the time-varying scattering channel and the transmitter pulse-shaping filter. Fig. 2.2 shows a 1/2-chip spaced square-root raised-cosine pulse-shape with 0.22 excess bandwidth. Fig. 2.3 shows the result of convolving the pulse-shape with a typical scattering channel. The channel is considered to be continuously time-varying; however, in some derivations we assume that the channel is fixed, which is approximately true over short time intervals. (see Appendix A for discussion of time-varying channel realizations and simulation duration)

2.3 Multichannel Received Signal

In this section we define notation of the multichannel received chip-rate signal. Multiple channels can be formed by either oversampling the received signal or by adding extra antennas to the receiver. Throughout this thesis, we borrow the notation for multiple channels from the book chapter by Johnson et al. [6].

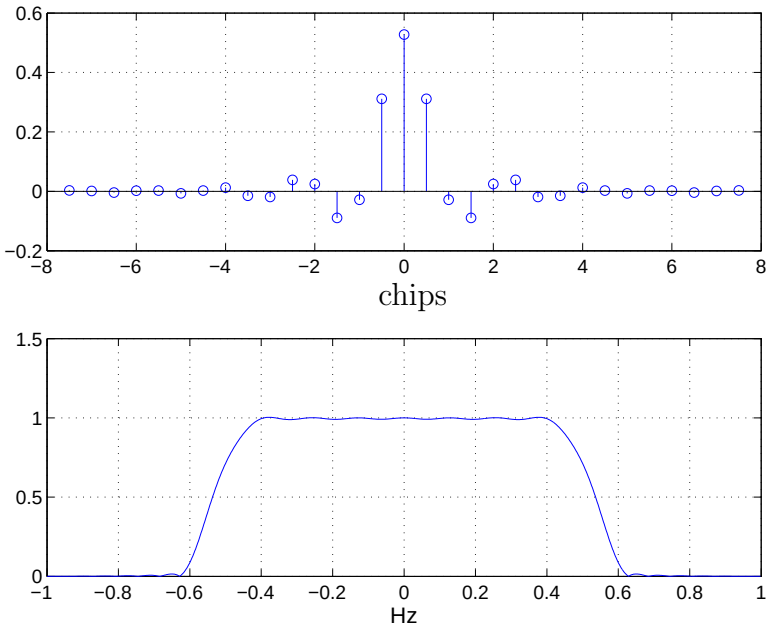

Figure 2.2: Square-root raised cosine pulse-shape and magnitude spectrum.

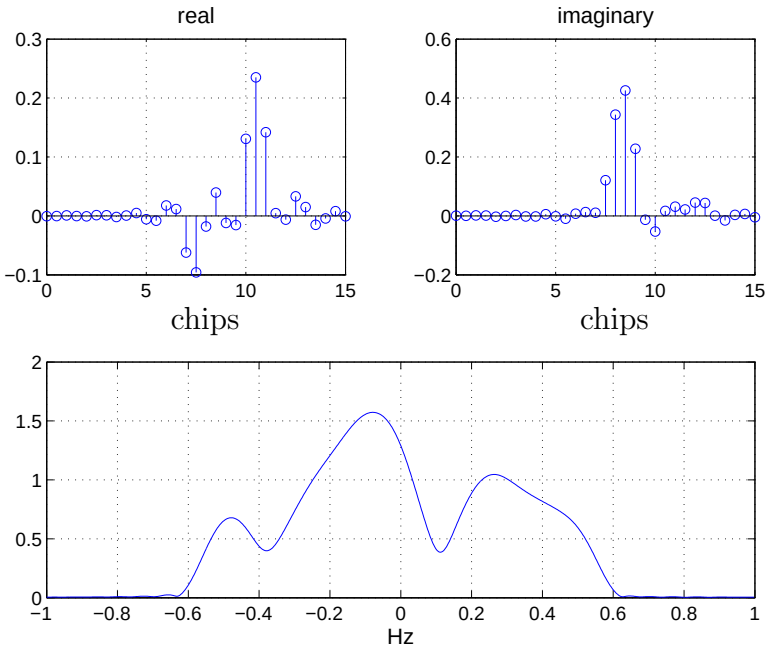

Figure 2.3: Pulse-shape convolved with channel.

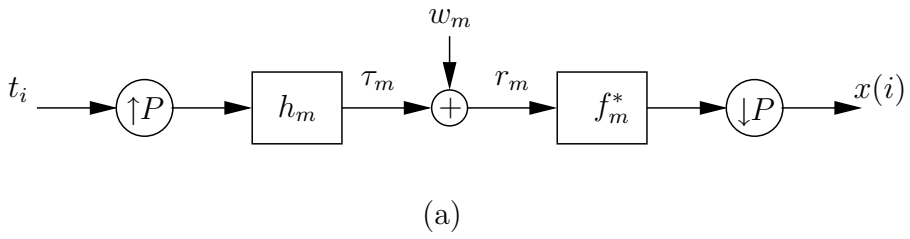

(a)

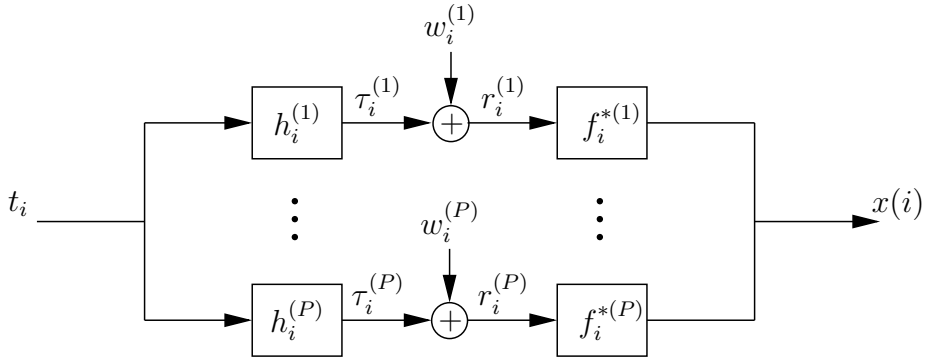

(b)

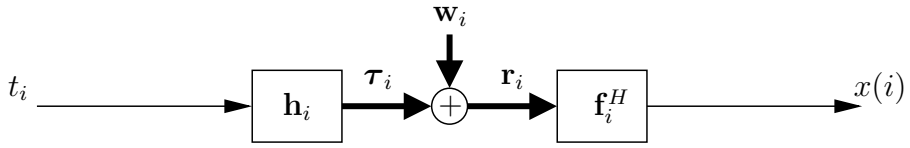

(c)

Figure 2.4: Fractional rate and multichannel representations.

Fig. 2.4(a) describes a discrete-time fractionally spaced channel model with sub-sampling of P samples per chip. The fractional-rate output r_m is written

$$r_m = \sum_{\ell} t_\ell h_{m-\ell P} + w_m \tag{2.5}$$

Assume h_m is finite duration, then we can write the channel in vector form:

$$\mathbf{h} = (h_0, h_1, \ldots, h_{(L_h+1)P-1})^T \tag{2.6}$$

where L_h denotes length of channel in chip intervals. We now sub-sample the channel and collect the phases into vectors in order to show equivalence to a multichannel model (Fig. 2.4(b)). Defining the p^{th} subchannel ($p \in \{1, \ldots, P\}$) quantities as

$$h_i^{(p)} := h_{(i+1)P-p}, \quad \tau_i^{(p)} := \tau_{(i+1)P-p}, \quad r_i^{(p)} := r_{(i+1)P-p}, \quad w_i^{(p)} := w_{(i+1)P-p}, \tag{2.7}$$

The vector-valued channel response at chip index i is

$$\mathbf{h}_i := \begin{bmatrix} h_i^{(1)} \\ \vdots \\ h_i^{(P)} \end{bmatrix} \tag{2.8}$$

and we can write the following equations for the received chip-rate signal

$$\boldsymbol{\tau}_i = \sum_{\ell=0}^{L_h} \mathbf{h}_\ell \, t_{i-\ell}, \quad \mathbf{r}_i = \boldsymbol{\tau}_i + \mathbf{w}_i \tag{2.9}$$

Using the above notation, the vector-valued multichannel block diagram (Fig. 2.4(c)) closely resembles a single-channel diagram.

2.4 Multichannel Chip-Rate FIR Linear Receiver

Given the past L_f+1 multichannel observations $\mathbf{r}_i$, a specially chosen finite impulse response (FIR) linear receiver produces a desired output. The goal of this thesis is

to devise algorithms to learn and track *optimal* filter coefficients. The chip-rate multichannel FIR receiver is defined

$$\mathbf{f}_i := \begin{bmatrix} f_i^{(1)} \\ \vdots \\ f_i^{(P)} \end{bmatrix} \quad i \in \{0, 1, \ldots, L_f\} \tag{2.10}$$

where $f_i^{(p)}$ are the coefficients of the p^{th} sub-filter in Fig. 2.4(b). The fractional-rate and multichannel FIR coefficients are connected by the relationship

$$f_{iP+p-1} = f_i^{(p)} \tag{2.11}$$

The FIR filter output $x(i)$ is given by

$$x(i) = \sum_{\ell} \mathbf{f}_\ell^H \mathbf{r}_{i-\ell} = \mathbf{f}^H \mathbf{r}(i) \tag{2.12}$$

where

$$\mathbf{f} := \begin{bmatrix} \mathbf{f}_0 \\ \vdots \\ \mathbf{f}_{L_f} \end{bmatrix} \quad \text{and} \quad \mathbf{r}(i) := \begin{bmatrix} \mathbf{r}_i \\ \vdots \\ \mathbf{r}_{i-L_f} \end{bmatrix} \tag{2.13}$$

The vector-valued received signal can be written

$$\underbrace{\begin{bmatrix} \mathbf{r}_i \\ \vdots \\ \mathbf{r}_{i-L_f} \end{bmatrix}}_{\mathbf{r}(i)} = \underbrace{\begin{bmatrix} \mathbf{h}_0 & \cdots & \mathbf{h}_{L_h} & & \\ & \ddots & & \ddots & \\ & & \mathbf{h}_0 & \cdots & \mathbf{h}_{L_h} \end{bmatrix}}_{\mathbf{H}} \underbrace{\begin{bmatrix} t_i \\ \vdots \\ t_{i-L_h-L_f} \end{bmatrix}}_{\mathbf{t}(i)} + \underbrace{\begin{bmatrix} \mathbf{w}_i \\ \vdots \\ \mathbf{w}_{i-L_f} \end{bmatrix}}_{\mathbf{w}(i)} \tag{2.14}$$

$$\mathbf{r}(i) = \mathbf{H}\mathbf{t}(i) + \mathbf{w}(i) \tag{2.15}$$

Thus the chip-rate multichannel FIR filter output is written

$$x(i) = \mathbf{f}^H \mathbf{H} \mathbf{t}(i) + \mathbf{f}^H \mathbf{w}(i) \tag{2.16}$$

$$= \mathbf{q}^H \mathbf{t}(i) + \tilde{w}(i) \tag{2.17}$$

$$= \sum_{\ell=0}^{L_f+L_h} q_\ell^* t_{i-\ell} + \tilde{w}(i) \tag{2.18}$$

where $\mathbf{q} = \mathbf{H}^H \mathbf{f}$ is the system response, and $\tilde{w}(i)$ is the filtered noise.

2.5 Literature Survey

In this section we provide a background of previous research that exploits properties of the scrambled CDMA downlink to design improved sub-optimal, low-complexity receivers. We have found that few papers contribute adaptive solutions. We stress once again that adaptive MAI-reducing receivers tailored for the un-scrambled (short-code, cyclo-stationary) CDMA system are not applicable to our problem, hence, will not be covered in this section. The notation of this section is self-contained.

Anja Klein [7] makes three basic assumptions downlink:

(A.1) All users' signals travel through the same channel to the receiver.

(A.2) Only the desired user's code is known by the receiver.

(A.3) Computational complexity should be low at the mobile.

Other papers assumed that all active codes are known at the receiver.

Using assumptions (A.1) and (A.2) she derives a minimum mean squared error (MMSE) equalizer. Her solution is simpler than the optimal multiuser detector, but the large matrix inversions required are still too complex for practical implementation in the near future.

Klein assumes a block-processing model. In her notation, users' data symbols are stacked into a tall vector, $\mathbf{b} = \left[\mathbf{b}^{(1)T}, \ldots, \mathbf{b}^{(K)T}\right]^T$, where $\mathbf{b}^{(k)}$ is a vector of the k^{th} user's symbols; and users' multi-rate spreading code sequences are lined up into a very wide matrix, $\mathbf{C} = \left[\mathbf{C}^{(1)}, \ldots, \mathbf{C}^{(K)}\right]$, where each user's spreading matrix is column

diagonal

$$\mathbf{C}^{(k)} = \begin{bmatrix} \mathbf{c}_1^{(k)} & & & \\ & \mathbf{c}_2^{(k)} & & \\ & & \ddots & \\ & & & \mathbf{c}_N^{(k)} \end{bmatrix}$$

and where $\mathbf{c}_n^{(k)}$ is the spreading code of the k^{th} user's n^{th} bit. Thus, the transmitted signal $\mathbf{t}$ is

$$\mathbf{t} = \mathbf{C}\mathbf{b}$$

and the received vector $\mathbf{r}$ is written

$$\mathbf{r} \;=\; \mathbf{H}\mathbf{t} + \mathbf{w}$$

where $\mathbf{w}$ is the additive noise; $\mathbf{H}$ is a convolution matrix,

$$\mathbf{H} = \begin{bmatrix} h_0 & & & \\ \vdots & h_0 & & \\ h_{L_h} & \vdots & \ddots & \\ & h_{L_h} & & h_0 \\ & & \ddots & \vdots \\ & & & h_{L_h} \end{bmatrix}$$

K is the number of users and L_h+1 is the number of paths in the channel multipath.

The matrix equalizer of the received multiuser chip signal, $\mathbf{r}$, according to the zero-forcing criterion is

$$\mathbf{F}_{\text{ZF}} \;=\; \left(\mathbf{H}^H\mathbf{H}\right)^{-1}\mathbf{H}^H \tag{2.19}$$

and the matrix equalizer of the received multiuser signal, $\mathbf{r}$, according to the minimum mean squared error (MMSE) criterion is

$$\mathbf{F}_{\text{MMSE}} \;=\; \left(\mathbf{H}^H\mathbf{H} + \sigma^2\mathbf{R}_{\mathbf{t}}^{-1}\right)^{-1}\mathbf{H}^H \tag{2.20}$$

where $\mathbf{R}_{\mathbf{t}} = \text{E}[\mathbf{t}\mathbf{t}^H]$. The derivation of (2.19) and (2.20) can be found in any standard text on parameter estimation (e.g., [8] pg. 155-157). The estimate of the desired

user's symbols is computed by multiplying the received vector by the equalizer matrix (zero-forcing (2.19) or MMSE (2.20)), and match filtering with the desired user's code matrix

$$\hat{\mathbf{b}}^{(k)} = \underbrace{\left(\text{diag}\left(\mathbf{C}^{(k)H}\mathbf{C}^{(k)}\right)\right)^{-1}}_{\text{normalization}} \mathbf{C}^{(k)H}\mathbf{F}\,\mathbf{r} \tag{2.21}$$

Klein simplifies the inversion of $\mathbf{R_t}$ in (2.20) by assuming $\mathbf{R_t} = \sigma_t^2\mathbf{I}$, which is true when a random scrambling code is applied at the transmitter; however, computing the inverses in (2.19) or (2.20) to form the block equalizer matrix for large block lengths is overtaxing and requires knowledge of the channel.

Klein's work is different from previous work in that she suggests to equalize the received chips prior to the despreading operation. In her work no attempt is made to form a channel estimate or to design an adaptive solution; all simulations assume perfectly known channel state information (CSI). The block equalizer was extensively studied with turbo and convolutional coding and decoding by Darwood et al. [9].

Ghauri and Slock state explicitly that the downlink signal is spread by orthogonal codes and scrambled by a long overlay sequence and that orthogonality of the Walsh-Hadamard short codes is destroyed when the signal passes through a multipath channel [10]. Their equalizers are multichannel and retain the goal of restoring the orthogonality of the users' signals so that MAI may be removed by despreading with the desired user's short code. They also determine the minimum equalizer length necessary to satisfy the zero-forcing criterion.

Slock is co-author of several subsequent papers relating to equalizing the CDMA downlink. Topics include the following: an intracell interference cancelling rake receiver [11], a semi-blind inter-cell interference canceller [12], a blind maximum SINR

receiver [13], an intercell interference canceller exploiting excess codes [14], a comparison of downlink transmit diversity schemes for rake and SINR maximizing receivers [15], and a rake structured SINR maximizing receiver [16].

Researchers associated with Nokia have contributed several papers to WCDMA downlink equalization. Werner and Lilleberg [17] make essentially the same assumptions as Ghauri and Slock [10] on the WCDMA downlink, but consider chip-spaced, rather than fractionally-spaced, equalizers. Werner and Lilleberg are first to suggest an adaptive solution, which is very similar to RLS. Nevertheless, their equalizers operate on blocks of received samples (identical to Klein [7]) and their numerical simulations consider only static channels. Several subsequent papers addressing simpler adaptive solutions emerged from Nokia with the following topics: chip-spaced Griffith's algorithm [18]; chip-spaced chip separation [19]; multichannel Griffith's algorithm and multichannel adaptive chip separation [20]; and modified Griffith's algorithm [21]. The Griffith's algorithm is a simple modification to LMS that relies on channel estimation.

Previous to their first long-code paper [17], researchers associated with Nokia had analyzed short-code CDMA downlink receivers [22], [23].

Frank and Visotsky (Motorola) independently introduced a paper on CDMA downlink equalization [24]. They also make assumptions (A.1)-(A.3) in presenting their equalizer, and analyze the SINR performance gains of the MMSE receiver with respect to the matched filter receiver. They suggest descrambling and despreading the equalizer output prior to generating the error signal, however, no adaptive simulations are performed.

Frank and Visotsky [25] extend their work in a paper coauthored with U. Madhow, in particular, they derive the scrambling-code dependent MMSE equalizer, and then average to obtain the average MMSE equalizer, which is the same theoretical equalizer studied in this thesis. Comparisons are made between equalizers for random and orthogonal spreading sequences, both with long overlay code, with the result that the average MMSE equalizer is identical for both cases. The MMSE equalizer is shown to suppress non-white additive noise, e.g., intercell interference, and extensive numerical simulations show the advantages of equalization over rake reception. It is shown that despreading the pilot using a shortened spreading factor, i.e., updating faster than symbol rate, is beneficial to tracking, which motivates us to look at methods to update at chip-rate. USPTO 6175588, which patents CDMA downlink equalizers, was filed by Frank, Visotsky, and Madhow prior to presenting their results of [24].

Krauss and Zoltowski, researchers at Purdue University, also contributed several papers on synchronous long-code CDMA equalization. They give zero-forcing conditions for a two channel equalizer and provide simulation studies comparing the zero-forcing equalizer to the rake receiver [26]. Later, they essentially combine the work of Ghauri and Slock [10] and Frank et al. [25], by presenting a multichannel MMSE equalizer, and compare the theoretical MMSE equalizer to the zero-forcing receiver and the rake receiver [27]. By the use of the matrix inverse lemma, they show that the average MMSE equalizer

$$\mathbf{f}_* = \sigma_t^2 \left[\sigma_t^2 \mathbf{H}^H \mathbf{H} + \sigma_w^2 \mathbf{I}\right]^{-1} \mathbf{H}^H \boldsymbol{e}_\nu \tag{2.22}$$

can be written as

$$\mathbf{f}_* = \sigma_t^2 \mathbf{H}^H \left[\sigma_t^2 \mathbf{H}\mathbf{H}^H + \sigma_w^2 \mathbf{I}\right]^{-1} \boldsymbol{e}_\nu \tag{2.23}$$

At low SNR the MMSE equalizer behaves like the matched filter receiver

$$\mathbf{f}_* \approx \mathbf{H}^H \boldsymbol{e}_\nu \tag{2.24}$$

and at high SNR it looks like the zero-forcing equalizer

$$\mathbf{f}_* \approx \mathbf{H}^H \left[\sigma_t^2 \mathbf{H}\mathbf{H}^H\right]^{-1} \boldsymbol{e}_\nu \tag{2.25}$$

The previous work at Purdue assumes that the channel is known at the receiver, but does not show how to determine the channel. A blind channel identification method based on the cross-relation method of Xu, Liu, Tong, and Kailath [28] is proposed, which makes use of multiple channels at the receiver [29]. Simulation studies, nevertheless, show that the performance of the channel identifier, when used to calculate the zero-forcing solution, is 15 dB away from the ideal zero-forcing solution; hence, better channel estimation is necessary to approach the ideal performance.

Krauss and Zoltowski compare multichannel diversity schemes obtained by either fractionally spaced sampling or by employing dual receive antennas [30]. They perform simulations of ideal rake, zero-forcing, and MMSE receivers on static channels and show that dual antenna diversity is superior to fractionally spaced diversity.

The MMSE and zero-forcing equalizers [30] are studied in the soft hand-off situation, which is characterized by the mobile simultaneously receiving data symbols from two base-stations, thus the receiver is subject to severe out-of-cell interference. The MMSE equalizer is shown to be robust in such cases due to its ability to suppress non-white interference. Simulations are performed with ideal MMSE and rake receivers [31] [32].

Chip-level, symbol-level, and subspace-constrained symbol-level MMSE equalizers are derived [33] [34]. The chip-level MMSE equalizer minimizes the mean squared

error (MSE) between the transmitted and received-equalized signal, the symbol-level MMSE equalizer minimizes the MSE between the bit estimate and the desired bit, and the subspace-constrained equalizer first projects the received signal prior to equalization onto a subspace spanned by shifted versions of the scrambling code, multiplied by the time-reversed desired user's code. Since the bit estimate is a function of the scrambling code, the symbol-level and subspace-constrained equalizers change from bit to bit. A few assumptions are made in order to simplify the computation of the symbol-level equalizer, however, simulations show that the symbol-level and subspace-constrained equalizers gain little in performance over the well known chip-level equalizer.

Chowdhury and Zoltowski study sparse equalization [35] [36] [37]. A block adaptive multistage nested wiener filter (MSNWF) is suggested and shown to have good convergence properties in the static channel case [35] [36]. Also, a method of projecting the observed signal onto a lower dimensional subspace prior to the MSNWF is shown to improve convergence. This method is called "semi-blind structured equalization." The sparsity of the channel implies that the channel/pulse-shape response lies in a space that is spanned by few columns of the pulse-shape convolution matrix. Knowledge of channel peak locations is required to determine the subspace. The semi-blind structured equalizer outperforms the pilot trained RLS and LMS equalizers on time-varying sparse channels [37].

L. Mailaender of Lucent studies efficient computation techniques of the MMSE equalizer assuming channel knowledge [38]. Mailaender assumes that the MMSE equalizer must be computed at the rate of the inverse of the time it takes the mobile

to traverse one-tenth wavelength. The computation techniques include the following: Block-Toeplitz, Polyphase, and Gauss-Seidel iterations. No fading simulations were performed.

Since practical calculation of the MMSE filter relies on channel estimates, and these estimates are likely to be very noisy, error effects on the calculation of the zero-forcing equalizer are studied [39]. It is found that pulse-shape mismatch at the receiver can have drastic effects on the calculation of the equalizer, and solutions are given to counter the mismatch.

A blind equalizer was developed by Li and Liu that satisfies the following criterion [40]:

$$\begin{aligned} \hat{\mathbf{f}} &= \arg \min_{\mathbf{f}} \mathrm{E} \left\| \mathbf{C}_o^H \mathbf{Y}(n) \mathbf{f} \right\|^2 \\ &\quad \text{subject to } \mathrm{E} \left\| \mathbf{c}_1^H \mathbf{Y}(n) \mathbf{f} \right\|^2 = 1 \end{aligned} \tag{2.26}$$

where $\mathbf{C}_o$ is the subspace orthogonal to the user codes, i.e., the excess codes; $\mathbf{c}_1$ is the desired user's code; and $\mathbf{Y}(n)\mathbf{f}$ is the equalized-received signal. An adaptive algorithm for training $\mathbf{f}$ is given. It is important to note that this algorithm works for short codes as well as for long codes because the chip-rate signal is equalized prior to the projection. The scrambling code used at the transmitter rotates the code-space from symbol to symbol, but the codes remain orthogonal because the scrambling operation is unitary. The blind equalizer (2.26) pushes the received energy back into the orthogonal code space in the direction of the desired user's code, so despreading can remove MAI. Slock and Ghauri show that the blind equalizer (2.26) maximizes SINR in the case of random scrambling codes [13].

A number of papers were produced by researchers at Interuniversity Micro-Electronics Center (IMEC) in Belgium. The same bit-rate updated pilot-trained RLS equalizer as Frank and Visotsky [25] is proposed, and fractionally-spaced equalization is shown to perform much better than baud-spaced equalization [41]. Later, a semi-blind approach is taken where an equalizer is found such that when the equalized-received signal is projected onto the subspace orthogonal to the users' codes, the projection is close to the pilot signal in a least squares sense [42]. Block processing and adaptive algorithms are derived that rely on a model with at least two receive channels. If pilot symbols are present in the desired user's bit stream then the semi-blind equalizer can be extended to this case [43]. The semi-blind equalizer was also studied in the context of soft hand-off mode [44], and extensive explanation of adaptive solutions were also undertaken [45]. The semi-blind methods are also generalized to the case of transmit-diversity in the downlink [46].

As early as 1993, Bottomley of Ericcson Inc. noticed that the rake receiver is suboptimal in a CDMA downlink because the intercell interference is colored by the same channel as the desired user [4]. The rake receiver (matched filter) is optimal only in single-symbol communications with additive white gaussian noise (AWGN). By assuming that the intracell interference is colored Gaussian noise, Bottomley derives a generalized rake receiver, which maximizes the SINR [47]. The rake-finger weights are precisely the solution to the MMSE equalizer. The generalized rake receiver is shown to also suppress colored intercell interference [48].

Monisha Ghosh of Phillips Research shows that the MMSE equalizer trained by despreading the pilot signal is suboptimal in the sense of maximizing the SINR in the

bit estimate of the desired user, but is reasonably close to optimal [49]. She suggests that multiplexing the pilot power over several codes instead of increasing the pilot power of a single code is better for tracking. An extension of her method would be to use decision directed equalization on all active codes, i.e., treat each user as a pilot.

A few decision feedback equalizer (DFE) methods have been proposed. The DFE of Roessler et al. (Fig. 2.5) first equalizes then decodes the received signal in order to provide reliable multiuser bit estimates to be re-spread and input into a delayed chip-level DFE for re-processing [1]. The decoding operation prior to re-spreading is necessary due to the unreliable bit estimates provided by a pilot-trained equalizer, which inadequately tracks the optimal equalizer. This work is similar to our delayed decision-directed scheme (Chapter 4), but their equalizer has disadvantages: each equalizer must be trained separately; twice must the data be decoded, hence, deep interleavers imply significant delays in final data output; and they consider chip-spaced–rather than fractionally-spaced–equalization. We suspect that adaptive implementations of the first (linear) equalizer stage will more than remove the 1 dB advantage of their delayed DFE, and we stress that Roessler et al. ignore issues of adaptivity in their work.

Yang and Li propose a DFE that exploits the finite alphabet of the desired user's transmitted symbols [50]. A single feedforward filter is used in conjunction with several feedback filters. In the case of BPSK, the possible values of the current symbol can only be either $+1$ or -1. There are two feedback paths. For one of these paths, the input is the code chips of the current symbol. For the other path, the input is the sign-inverted code chips of the current symbol. The outputs of these two paths

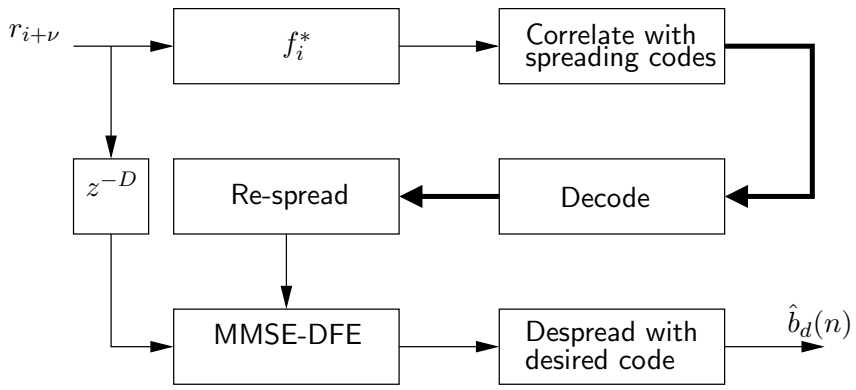

Figure 2.5: DFE block diagram of Roessler et al [1].

are further de-spread separately. A minimum distance decoder is used that decides in favor of +1 if the despread signal corresponding to the first path is closer to +1 than the output of the despread second path is to −1. No adaptive solution is given and the channel is assumed to be perfectly known. Their method does not scale well since the number of feedback paths is M^N, where M is the number of symbols in the alphabet and N is the number of desired bit-streams. The simulations are performed with static known channels and the DFE performs better than the linear MMSE receiver. However, as the number of users increases the performance gap decreases between the DFE and the linear receiver.

It has been shown that many researchers have tackled the problem of improving the CDMA downlink. Adaptive blind, semi-blind, and trained methods have been studied. However, we are unaware of previous work that mirrors the adaptive solutions set forth in this thesis.

CHAPTER 3

LINEAR EQUALIZATION

3.1 Bit Estimates

The purpose of this section is to derive bit estimates and show that equalizing the signal reduces multi-access interference (MAI) with respect to the matched filter (rake) receiver. We advance the received-equalized signal $x(i)$ by ν (the forced system delay) for notational convenience in writing the bit estimates. Fig. 3.1(a.) shows the familiar coherent rake receiver, which linearly combines several fingers using combining weights $\mathbf{f}^H$. Fig. 3.1(b.) is equivalent to Fig. 3.1(a.) assuming the equalizer coefficients $\mathbf{f}^H$ are held constant over bit intervals. From Fig. 3.1(b.), we see that ν can be thought of as the forced delay of the combined channel-equalizer response and the choice of ν will affect equalizer performance. In rake combining, $\nu = L_h + 1$, $\mathbf{f}_i = \mathbf{h}_{L_h - i}$ and $L_f = L_h$.

If we define the system response $\{q_i\}$ and filtered noise $\tilde{w}(i)$ by (2.18), then using (2.1), the equalizer output can be written

$$\begin{aligned} x(i+\nu) &= \tilde{w}(i+\nu) + \sum_{\ell=0}^{L_h+L_f} q_\ell^* \, t(i+\nu-\ell) \\ &= \tilde{w}(i+\nu) + \sum_{\ell=0}^{L_h+L_f} q_\ell^* \, s(i+\nu-\ell) v(i+\nu-\ell) \end{aligned} \tag{3.1}$$

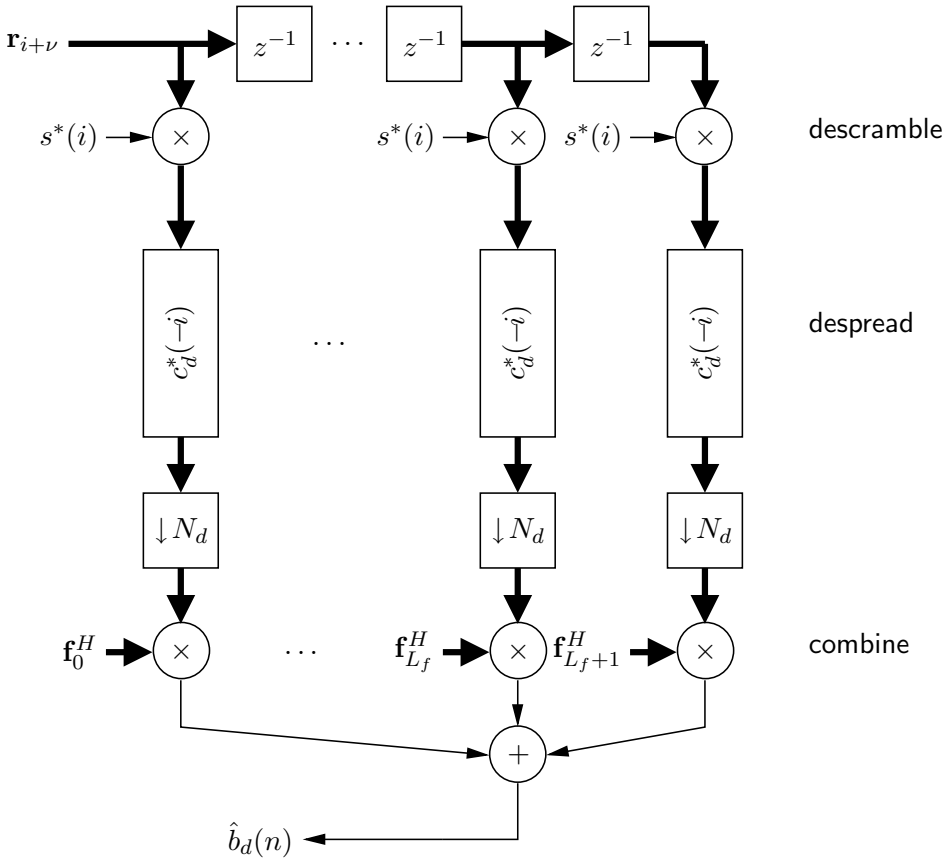

(a)

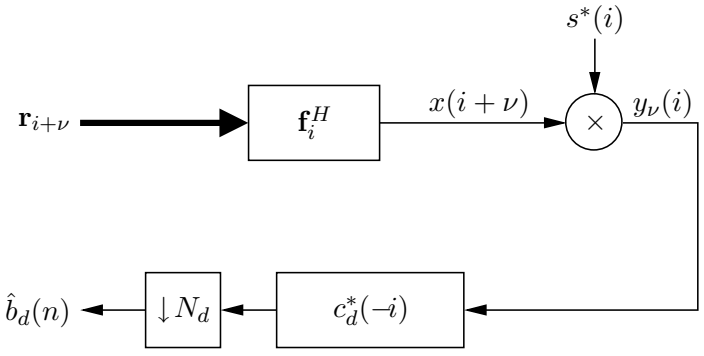

(b)

Figure 3.1: Equivalent structures of (a) rake and (b) equalizer for detection of d^{th} user's bits.

From Fig. 3.1(b.) and A.1), the descrambled signal $\{y_\nu(i)\}$ can be written as

$$\begin{aligned} y_\nu(i) &= s^*(i)\tilde{w}(i+\nu) + q_\nu^* v(i) \\ &\quad + \sum_{\ell\neq\nu} q_\ell^* s^*(i) s(i+\nu-\ell) v(i+\nu-\ell) \end{aligned} \tag{3.2}$$

The first term on the right of (3.2) is additive noise, the second term the desired signal plus "coherent" MAI and pilot, and the third "randomized" interference.

From Fig. 3.1 and A.2), the bit estimates for user d (desired) are obtained by despreading (3.2) with the d^{th} user's short code and downsampling by N_d.

$$\begin{aligned} \hat{b}_d(n) &= \sum_j c_d^*(-j) y_\nu(nN_d - j) \\ &= \sum_{i=0}^{N_d-1} c_d^*(i) y_\nu(nN_d + i) \\ &= \sum_{i=0}^{N_d-1} c_d^*(i) s^*(nN_d+i)\tilde{w}(nN_d+i+\nu) + q_\nu^* b_d(n) \\ &\quad + \sum_{\ell\neq\nu} q_\ell^* \sum_{i=0}^{N_d-1} s^*(nN_d+i) s(nN_d+i+\nu-\ell) \\ &\quad \cdot c_d^*(i) v(nN_d+i+\nu-\ell) \end{aligned} \tag{3.3}$$

From (3.3) we see that $\hat{b}_d(n)$ is composed of a noise term, a signal term, and an interference term. The interference term vanishes if and only if the channel is perfectly equalized, i.e., $q_i = \delta_{i-\nu}$ for some ν. From this observation we conclude:

- For non-trivial channels, a matched filter produces MAI-corrupted estimates.
- For perfectly-equalized or trivial channels $q_i = \delta(i-\nu)$, the MAI vanishes.

The drawback of equalization is the potential for noise gain, i.e., increase in the variance of $\tilde{w}(i)$ relative to w_m, as might occur if the channel has a deep spectral null. This can be ameliorated through the use of minimum mean-squared error (MMSE)

rather than zero-forcing (ZF) equalization, thus compromising MAI reduction for noise amplification. In the end, if we assume that the MAI power is much greater than the noise power, the MAI-reduction potential of equalization should outweigh the loss incurred by noise gain. These issues have been explored in detail (for various channels and user loadings) throughout the literature (see [27]).

3.2 Theoretical MMSE Chip Equalizer

3.2.1 Multiuser-Trained Equalizer

The optimal fractionally spaced equalizer (FSE) according to the minimum mean squared error (MMSE) criterion is the filter, $\mathbf{f}$, which minimizes the cost

$$J_t^{(\nu)} = \mathrm{E}\left|\mathbf{f}^H\mathbf{r}(i+\nu) - t(i)\right|^2$$

and is given by (derivation inAppendix B)

$$\mathbf{f}_{t,*}^{(\nu)} = \sigma_t^2\left(\sigma_t^2\mathbf{H}\mathbf{H}^H + \sigma_w^2\mathbf{I}\right)^{\dagger}\mathbf{H}\mathbf{e}_\nu \tag{3.4}$$

where $\mathbf{r}(i)$, $\mathbf{H}$, and $\mathbf{f}$ are defined in Section 2.4; $\mathbf{e}_\nu = \left[0\ldots0,1,0\ldots0\right]^T$, i.e., $\mathbf{e}_\nu$ is the unit vector with a one in the ν^{th} position, ($\nu \geq 0$); and $(\cdot)^\dagger$ denotes the Moore-Penrose pseudo-inverse [51].

If the total transmitted signal $t(i)$ is available for training, we may use the standard LMS algorithm to adaptively learn and track (3.4) in time-varying channel conditions. In the CDMA systems under consideration, however, training comes in the form of a code-multiplexed pilot signal. In other words, the transmitted signal consists of a continuously-transmitted training signal superimposed with unknown user signals.

3.2.2 Pilot-Trained Equalizer

Due to A.3), a chip-rate error signal is readily constructed as the difference between the descrambled equalizer output and a constant reference value, say γ

$$J_p^{(\nu)} = \mathrm{E}\left|s^*(i)\mathbf{f}^H\mathbf{r}(i+\nu) - \gamma\right|^2 \tag{3.5}$$

which has MMSE solution (derivation inAppendix B)

$$\mathbf{f}_{p,*}^{(\nu)} = \gamma^* \frac{b_0}{\sqrt{N_0}} \left(\sigma_t^2 \mathbf{H}\mathbf{H}^H + \sigma_w^2 \mathbf{I}\right)^\dagger \mathbf{H}\mathbf{e}_\nu \tag{3.6}$$

Hence choosing

$$\gamma = \frac{\sigma_t^2}{\frac{b_0^*}{\sqrt{N_0}}} \tag{3.7}$$

sets $\mathbf{f}_{t,*}^{(\nu)} = \mathbf{f}_{p,*}^{(\nu)}$, i.e., proper choice of γ implies that a pilot-trained adaptive LMS equalizer will converge in the mean to the MMSE equalizer given by (3.4).

3.3 SINR Calculation

In this section we calculate the signal to interference plus noise ratio (SINR) of the equalized bit estimate (3.3), given the equalizer weights and channel state information. We assume that the channel is static, which would be the case over short periods of time, in which case the SINR calculation may be thought of as instantaneous average SINR. Expectations are taken over the user bits, the scrambling code, and the additive noise.

Without loss of generality, the bit estimate of the 0^{th} bit of the d^{th} user is

$$\begin{aligned}\hat{b}_d(0) &= \sum_{i=0}^{N_d-1} c_d^*(i)s^*(i)\tilde{w}(i+\nu) + q_\nu^* b_d(0) \\ &\quad + \sum_{\ell\neq\nu} q_\ell^* \sum_{i=0}^{N_d-1} s^*(i)s(i-\ell+\nu)c_d^*(i)v(i-\ell+\nu)\end{aligned}$$

Thus, the average SINR may be written

$$\frac{\mathrm{E}\,|q_\nu^* b_d(0)|^2}{\mathrm{E}\left|\sum_{i=0}^{N_d-1} c_d^*(i)s^*(i)\tilde{w}(i+\nu) + \sum_{\ell\neq\nu} q_\ell^* \sum_{i=0}^{N_d-1} s^*(i)s(i-\ell+\nu)\cdot c_d^*(i)v(i-\ell+\nu)\right|^2} \tag{3.8}$$

The power in the equalized-descrambled-despread noise is

$$\begin{aligned}
\mathrm{E}\left|\sum_{i=0}^{N_d-1} c_d^*(i)s^*(i)\tilde{w}(i+\nu)\right|^2 &= \sum_{i=0}^{N_d-1}\sum_{i=0}^{N_d-1} c_d^*(i)c_d(j)\underbrace{\mathrm{E}[s^*(i)s(j)]}_{=0,\ i\neq j} \\
&\quad \cdot \mathrm{E}[\tilde{w}(i+\nu)\tilde{w}(j+\nu)] \\
&= \sum_{i=0}^{N_d-1} \frac{1}{N_d}\,\mathrm{E}\,|\tilde{w}(i+\nu)|^2
\end{aligned}$$

where the equalized noise power is found from A.5) to be

$$\begin{aligned}
\mathrm{E}\,|\tilde{w}(i+\nu)|^2 &= \mathrm{E}\left|\mathbf{f}^H\mathbf{w}(i+\nu)\right|^2 \\
&= \mathbf{f}^H\,\mathrm{E}\left[\mathbf{w}(i+\nu)\mathbf{w}^H(i+\nu)\right]\mathbf{f} \\
&= \sigma_w^2\|\mathbf{f}\|^2
\end{aligned}$$

therefore, the equalized-descrambled-despread noise power is

$$\sigma_w^2\|\mathbf{f}\|^2 \tag{3.9}$$

Next, we find the power of the interference

$$\begin{aligned}
&\mathrm{E}\left|\sum_{\ell\neq\nu} q_\ell^* \sum_{i=0}^{N_d-1} s^*(i)s(i+\nu-\ell)c_d^*(i)v(i+\nu-\ell)\right|^2 = \\
&\qquad \sum_{\ell\neq\nu}\sum_{n\neq\nu} q_\ell^* q_n \sum_{i=0}^{N_d-1}\sum_{j=0}^{N_d-1} \underbrace{\mathrm{E}[s^*(i)s(i+\nu-\ell)s(j)s^*(j+\nu-n)]}_{=\begin{cases}1 & \text{if } \ell=n,\ i=j\\ 1 & \text{if } \ell=n=\nu,\ i\neq j\\ 0 & \text{else}\end{cases}} \\
&\qquad \cdot c_d^*(i)c_d(j)\,\mathrm{E}\left[v(i+\nu-\ell)v^*(j+\nu-n)\right] \\
&= \sum_{\ell\neq\nu} |q_\ell|^2 \sum_{i=0}^{N_d-1} |c_d(i)|^2\,\mathrm{E}\,|v^*(j+\nu-n)|^2 \\
&= \sigma_t^2 \sum_{\ell\neq\nu} |q_\ell|^2 \qquad (3.10)
\end{aligned}$$

Since the noise and interference in the denominator of (3.8) are uncorrelated, we use (3.9) and (3.10) to write

$$\mathrm{SINR} \;=\; \frac{P_d|q_\nu|^2}{\sigma_w^2\|\mathbf{f}\|^2 + \sigma_t^2\sum_{\ell\neq\nu}|q_\ell|^2} \qquad (3.11)$$

It is interesting to note that because of the random scrambling code, (3.11) depends on the bit energy of the desired user–not on the desired user's spreading factor.

3.4 Averaged-error LMS

In typical bit-rate equalizer update schemes, the equalized signal is descrambled and then despread by the pilot code to generate soft pilot-bit estimates. Soft errors can then be calculated (once per bit) and used for equalizer adaptation. When perfectly equalized, the recovered user signals are orthogonal and hence the bit-rate equalizer updates are free of MAI. Before equalizer convergence, however, the recovered users signals are not orthogonal, hence the equalizer updates are corrupted by MAI.

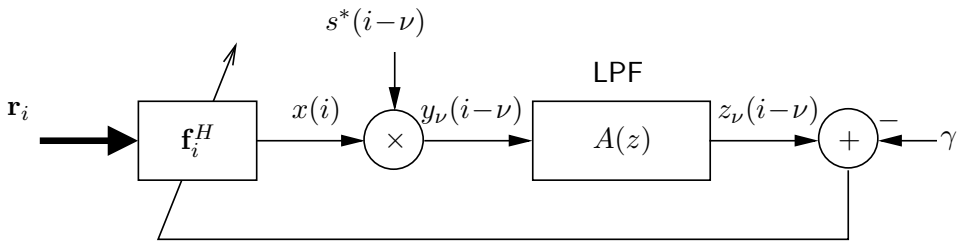

Figure 3.2: Chip-rate equalizer adaptation using filtered error.

Relative to bit-rate updating, chip-rate updating increases the update rate but employs an error signal corrupted by significantly higher levels of MAI. Nevertheless, the error-signal MAI is zero-mean and can be attenuated through lowpass filtering as shown in Fig. 3.2. The filter bandwidth should be optimized for a particular rate of channel variation and user load since lowering the cutoff frequency reduces MAI but slows the reaction of the error signal. From Fig. 3.2, the instantaneous error signal can be written

$$\hat{J}_{av}(i) \;=\; |z_\nu(i) - \gamma|^2 \tag{3.12}$$

Stochastic gradient descent of (3.12) can be accomplished using the chip-rate equalizer update

$$\mathbf{f}(i{+}1) \;=\; \mathbf{f}(i) - \mu \cdot \nabla_{\mathbf{f}(i)} \hat{J}_{av}(i{-}\nu) \tag{3.13}$$

where we have delayed the cost for reasons of causality. It is now left to find $\nabla_{\mathbf{f}(i)} \hat{J}_{av}(i)$.

Frank et al. [25] despread the pilot prior to generating an error signal (at bit-rate) in hopes of reducing MAI. They point out that tracking is enhanced when equalizer update-rate is increased by despreading with shorter spreading factor. This is possible

because the pilot bits are constant and spread with the all-ones code. We replace the pilot-code despread-downsample operation with a variable-bandwidth chip-rate averaging filter $A(z)$ to maintain balance between MAI reduction and channel-tracking performance. The averaging operation effectively despreads the received-equalized-descrambled signal to remove MAI, and updates come at chip-rate to improve tracking. An averaging filter $A(z)$ with very long impulse response (narrow bandwidth) would suit a static channel environment, but would suffer tracking errors under a time-varying channel. We suggest a recursive averaging filter structure to enable this trade-off.

3.4.1 Recursive Averaging

Suppose $A(z) = \frac{\zeta}{1-G(z)}$ where ζ is a constant, where $A(z)$ and $G(z)$ have real valued coefficients, and where $G(z)$ is strictly causal. Define $z(i) := z_\nu(i)$ and $y(i) := y_\nu(i)$ and say $z(i)$ is obtained recursively such that

$$\begin{aligned} z(i) &= \zeta y(i) + \sum_{j=1}^{L_g} g_j z(i-j) \\ &= \zeta \sum_{\ell=0}^{L_f} \mathbf{f}_\ell^H(i+\nu)\mathbf{r}_{i-\ell+\nu}s^*(i) + \sum_{j=1}^{L_g} g_j z(i-j) \end{aligned}$$

where we substituted from (2.12). To derive the gradient, we realize that

$$\nabla_{\mathbf{f}_\ell(i+\nu)}\hat{J}_{av}(i) = \big(z(i)-\gamma\big)^* \nabla_{\mathbf{f}_\ell(i+\nu)} z(i)$$

We define, for $0 \leq \ell \leq L_f$,

$$\boldsymbol{\alpha}_\ell(i+\nu) := \nabla_{\mathbf{f}_\ell(i+\nu)} z(i)$$

If we assume, due to small μ, that $\mathbf{f}_\ell^*(i+\nu) \approx \mathbf{f}_\ell^*(i+\nu-j)$, for $j \in \{1,\ldots,L_g\}$ then

$$\nabla_{\mathbf{f}_\ell(i+\nu)} z(i-j) \approx \nabla_{\mathbf{f}_\ell(i-j+\nu)} z(i-j) = \boldsymbol{\alpha}_\ell(i+\nu-j) \quad j \in \{1,\ldots,L_g\}$$

and we obtain the recursion

$$\boldsymbol{\alpha}_\ell(i+\nu) \;=\; \zeta \boldsymbol{r}_{i+\nu-\ell}\, s^*(i) + \sum_{j=1}^{L_g} g_j\, \boldsymbol{\alpha}_\ell(i+\nu-j) \tag{3.14}$$

Note that $\boldsymbol{\alpha}_\ell(i)$ is obtained by delaying the multichannel received signal $\mathbf{r}_i$ by ℓ, then de-scrambling and filtering with $A(z)$.

Defining $\boldsymbol{\alpha}(i) = [\boldsymbol{\alpha}_0(i), \ldots, \boldsymbol{\alpha}_{L_f}(i)]^T$, the equalizer update is

$$\mathbf{f}(i+1) \;=\; \mathbf{f}(i) - \mu \cdot \boldsymbol{\alpha}(i)\big(z(i-\nu)-\gamma\big)^* \tag{3.15}$$

where $\boldsymbol{\alpha}(i)$ is computed from (3.14).

By using a single-pole lowpass filter, i.e., $A(z) = \frac{1-\rho}{1-\rho z^{-1}}$, the filter bandwidth can be made readily adjustable, and the resulting algorithm takes the form

$$\begin{aligned}
\boldsymbol{\alpha}(i) &= (1-\rho)\mathbf{r}(i)s^*(i-\nu) \\
&\quad +\rho\boldsymbol{\alpha}(i-1) && (3.16)\\
e(i) &= (1-\rho)\left(\mathbf{f}^H(i)\mathbf{r}(i)s^*(i-\nu)-\gamma\right) \\
&\quad +\rho e(i-1) && (3.17)\\
\mathbf{f}(i+1) &= \mathbf{f}(i) - \mu\boldsymbol{\alpha}(i)e^*(i) && (3.18)
\end{aligned}$$

As is evident from (3.16)-(3.18), the incorporation of single-pole "matched filtering" is a form of filtered-error/filtered-regressor LMS [52]. This particular algorithm can be described as a third-order dynamical system, which has known advantages over standard (first-order) LMS in regards to tracking a Rayleigh-fading channel [53]. The tracking behavior of this algorithm is a function of two adjustable parameters, μ and ρ. Simulation studies under various operating conditions suggest that fixing ρ (within a suitable range) and adjusting μ yields performance very close to that

obtained through joint optimization of both parameters. (See Fig. 3.3). Given the operating conditions, a look-up table for determining the value of μ could be used while keeping ρ fixed, or an adaptive step-size algorithm could track μ.

Choice of μ and ρ could also depend on the desired user's spreading factor. If the system response (2.18) is time varying, then another noise term, depending on the amount of variation, will appear in the bit estimate (3.3). Users with short spreading factors will be less affected by high variation, hence, can tolerate more variation (e.g., larger μ and smaller ρ) to ensure better channel tracking.

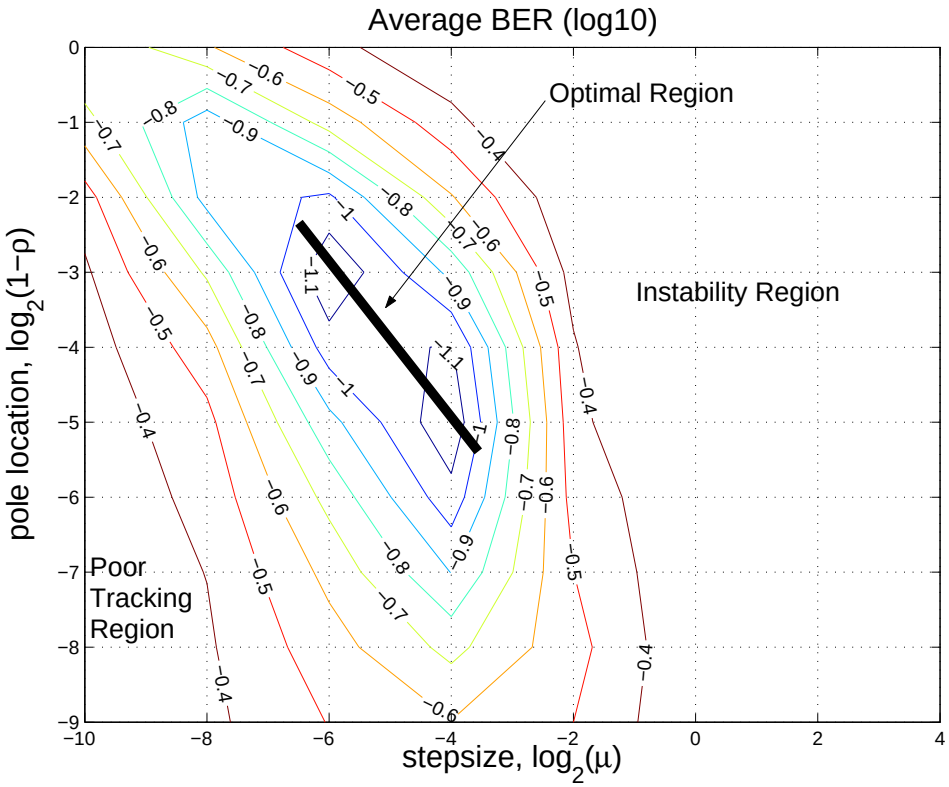

Figure 3.3: BER of bit-estimates versus equalizer pole location and stepsize.

3.4.2 Non-Recursive Averaging

Using arguments similar those in Section 3.4.1, it can be shown that, in the case of an FIR low-pass filter $\{a_i\}$, (3.15) defines the equalizer update recursion while (3.14) becomes

$$\boldsymbol{\alpha}_\ell(i) \;=\; \sum_{j=0}^{M_a-1} a_j \mathbf{r}_{i+\nu-j-\ell} s^*(i-j) \tag{3.19}$$

As before, $\boldsymbol{\alpha}_\ell(i)$ is obtained by delaying the multichannel received signal by ℓ, then de-scrambling and filtering.

3.5 Equalizer Analysis

Now that we have determined the equalizer update equation (3.15), we are interested in studying its mean convergence behavior. We show that the averaged-error LMS algorithm converges to the MMSE equalizer. BER and SINR performance of (3.16)-(3.18) are shown in Section 4.2.

3.5.1 Steady-State Behavior

To find the stationary points of the algorithm, we take the expectation of (3.15) and examine the limit as $i \to \infty$

$$\mathrm{E}\{\mathbf{f}(i+1)\} \;=\; \mathrm{E}\{\mathbf{f}(i)\} - \mu\,\mathrm{E}\{\boldsymbol{\alpha}(i)(z(i-\nu)-\gamma)^*\} \tag{3.20}$$

Let $\{a_i\}$ be the impulse response of the averaging filter $A(z)$ (see Fig. 3.2). Borrowing from Section 2.4, we have the following quantities:

$$\begin{aligned}
\boldsymbol{\alpha}(i) &= \sum_j a_j \mathbf{r}(i+\nu-j)s^*(i-j) \\
z(i) &= \sum_j a_j \mathbf{f}^H(i+\nu-j)\mathbf{r}(i+\nu-j)s^*(i-j) \\
\mathbf{r}(i) &= \mathbf{H}\mathbf{t}(i) + \mathbf{w}(i) \\
\mathbf{t}(i) &= \mathrm{diag}\{\mathbf{s}(i)\}\mathbf{v}(i) \\
\mathbf{v}(i) &= \mathbf{u}(i) + \frac{b_0}{\sqrt{N_0}}\mathbf{1}
\end{aligned} \tag{3.21}$$

where $\mathbf{u}(i) = [u(i), u(i-1), \ldots, u(i-L_h-L_f)]^T$; $\mathbf{s}(i) = [s(i), s(i-1), \ldots, s(i-L_h-L_f)]^T$; and $\mathbf{1}$ is the all ones vector. For a moment we concentrate on $\mathrm{E}\big\{\boldsymbol{\alpha}(i+\nu)z^*(i)\big\}$,

$$\begin{aligned}
&\mathrm{E}\big\{\boldsymbol{\alpha}(i+\nu)z^*(i)\big\} \\
&\quad = \sum_j \sum_\ell a_j a_\ell \,\mathrm{E}\left[\mathbf{r}(i+\nu-j)\mathbf{r}^H(i+\nu-\ell)s^*(i-j)s(i-\ell)\right] \mathrm{E}\left[\mathbf{f}(i+\nu-\ell)\right]
\end{aligned} \tag{3.22}$$

where we have made the small μ assumption that the parameters change slowly compared to the instantaneous input. Using A.1), A.4), and A.5),

$$\begin{aligned}
&\mathrm{E}\left[\mathbf{r}(i+\nu-j)\mathbf{r}^H(i+\nu-\ell)s^*(i-j)s(i-\ell)\right] \\
&\quad = \mathbf{H}\,\mathrm{E}\left[\mathbf{t}(i+\nu-j)\mathbf{t}^H(i+\nu-\ell)s^*(i-j)s(i-\ell)\right]\mathbf{H}^H \\
&\qquad + \mathrm{E}\left[\mathbf{w}(i+\nu-j)\mathbf{w}^H(i+\nu-\ell)\right] \underbrace{\mathrm{E}\left[s^*(i-j)s(i-\ell)\right]}_{=\begin{cases}1 & \text{if } j=\ell \\ 0 & \text{else}\end{cases}} \\
&\quad = \mathbf{H}\,\mathrm{E}\left[\mathbf{t}(i+\nu-j)\mathbf{t}^H(i+\nu-\ell)s^*(i-j)s(i-\ell)\right]\mathbf{H}^H + \sigma_w^2\mathbf{I}\,\delta_{j-\ell}
\end{aligned} \tag{3.23}$$

Now,

$$\begin{aligned}
&\mathrm{E}\left[\mathbf{t}(i+\nu-j)\mathbf{t}^H(i+\nu-\ell)s^*(i-j)s(i-\ell)\right] \\
&\quad = \mathrm{E}\left[\mathrm{diag}\{\mathbf{s}(i+\nu-j)\}\mathbf{v}(i+\nu-j)\mathbf{v}^H(i+\nu-\ell)\,\mathrm{diag}\{\mathbf{s}^H(i+\nu-\ell)\}s^*(i-j)s(i-\ell)\right]
\end{aligned} \tag{3.24}$$

and the $[a,b]^{th}$ element of (3.24) is

$$\mathrm{E}\left[v(i+\nu-j-a)v^*(i+\nu-\ell-b)\right]\underbrace{\mathrm{E}\left[s(i+\nu-j-a)s^*(i+\nu-\ell-b)s^*(i-j)s(i-\ell)\right]}$$
$$=\begin{cases}1 & \text{if } a=b, j=\ell \\ 1 & \text{if } a=b=\nu, j\neq\ell \\ 0 & \text{else}\end{cases} \tag{3.25}$$

Hence, (3.24) can be written

$$\sigma_t^2\mathbf{I}\,\delta_{j-\ell} + (1-\delta_{j-\ell})\mathbf{e}_\nu\mathbf{e}_\nu^H\,\mathrm{E}\left[v(i-j)v^*(i-\ell)\right] \tag{3.26}$$

Substituting (3.26) into (3.23), and substituting (3.23) into (3.22), we obtain

$$\begin{aligned}
\mathrm{E}\{\boldsymbol{\alpha}(i+\nu)z^*(i)\} &= \sum_j\sum_\ell a_j a_\ell\Big\{\sigma_t^2\mathbf{H}\mathbf{H}^H\,\delta_{j-\ell} + \sigma_w^2\mathbf{I}\,\delta_{j-\ell} \\
&\quad +(1-\delta_{j-\ell})\mathbf{h}_\nu\mathbf{h}_\nu^H\,\mathrm{E}\left[v(i-j)v^*(i-\ell)\right]\Big\}\,\mathrm{E}\left[\mathbf{f}(i+\nu-\ell)\right]
\end{aligned} \tag{3.27}$$

where $\mathbf{h}_\nu = \mathbf{H}\mathbf{e}_\nu$

Let us examine $\sum_j\sum_\ell a_j a_\ell\,\mathrm{E}\left[v(i-j)v^*(i-\ell)\right]$. Using A.3) and A.4)

$$\begin{aligned}
\sum_j\sum_\ell a_j a_\ell\,\mathrm{E}\left[v(i-j)v^*(i-\ell)\right] &= \sum_j\sum_\ell a_j a_\ell\frac{P_0}{N_0} \\
&\quad +\sum_j\sum_\ell a_j a_\ell\,\mathrm{E}\left[u(i-j)u^*(i-\ell)\right] \\
&= \frac{P_0}{N_0}\left(\sum_j a_j\right)^2 + \underbrace{\mathrm{E}\left|\tilde{u}(i)\right|^2}_{\sigma_{\tilde{u}}^2(i)}
\end{aligned} \tag{3.28}$$

where $\tilde{u}(i) = \sum_j a_j u(i-j)$. The aggregate multiuser signal $u(i)$ is non-white and cyclostationary with period of the lowest spreading factor if the system is employing non-random channelization codes such as Hadamard codes. However, averaging $u(i)$ with $\{a_i\}$ tends to remove the cyclostationarity, and we may approximate the generally time-varying quantity $\sigma^2_{\tilde{u}}(i)$ as static $\sigma^2_{\tilde{u}}$. Furthermore, if the spreading factors of the dominant users fit within the non-negligible portion of the impulse response $\{a_i\}$ then $u(i)$ is approximately despread, and the term $\sigma^2_{\tilde{u}}$ is small.

Next we find $\mathrm{E}\{\boldsymbol{\alpha}(i+\nu)\}$

$$\begin{aligned}
\mathrm{E}\{\boldsymbol{\alpha}(i+\nu)\} &= \sum_j a_j \mathrm{E}[\mathbf{r}(i+\nu-j)s^*(i-j)] \\
&= \sum_j a_j \mathbf{H}\,\mathrm{E}[\mathbf{t}(i+\nu-j)s^*(i-j)] + \underbrace{\mathrm{E}[\mathbf{w}(i+\nu-j)]\,\mathrm{E}[s^*(i-j)]}_{0} \\
&= \sum_j a_j \mathbf{H}\,\mathrm{E}[\mathrm{diag}\{\mathbf{s}(i+\nu-j)\}s^*(i-j)]\,\mathrm{E}\left[\mathbf{u}(i) + \frac{b_0}{\sqrt{N_0}}\mathbf{1}\right] \\
&= \sum_j a_j \mathbf{H}\,\mathrm{diag}\{\mathbf{e}_\nu\}\frac{b_0}{\sqrt{N_0}}\mathbf{1} \\
&= \sum_j a_j \frac{b_0}{\sqrt{N_0}}\mathbf{h}_\nu
\end{aligned} \tag{3.29}$$

Now let $i \to \infty$ and denote $\mathbf{f}(\infty) := \lim_{i\to\infty} \mathrm{E}[\mathbf{f}(i)]$. Hence

$$\begin{aligned}
\lim_{i\to\infty} \mathrm{E}\big\{\boldsymbol{\alpha}(i+\nu)z^*(i)\big\} \approx \Bigg[&\underbrace{\sum_j a_j^2\left(\sigma_t^2\mathbf{H}\mathbf{H}^H + \sigma_w^2\mathbf{I}\right)}_{\mathbf{B}^{-1}} \\
&+ \underbrace{\left(\frac{b_0}{\sqrt{N_0}}\left(\sum_j a_j\right)^2 + \sigma^2_{\tilde{u}} - \sum_j a_j^2\sigma_t^2\right)}_{\beta}\mathbf{h}_\nu\mathbf{h}_\nu^H\Bigg]\mathbf{f}(\infty)
\end{aligned} \tag{3.30}$$

and

$$\lim_{i\to\infty} \mathrm{E}\big\{\boldsymbol{\alpha}(i+\nu)\big\} = \sum_j a_j \frac{b_0}{\sqrt{N_0}}\mathbf{h}_\nu \tag{3.31}$$

Now we are in a position to calculate (3.20) as $i \to \infty$ and solve for $\mathbf{f}(\infty)$

$$\begin{aligned} \mathbf{f}(\infty) &= \mathbf{f}(\infty) - \mu \lim_{i\to\infty} \mathrm{E}\{\boldsymbol{\alpha}(i)(z(i-\nu)-\gamma)^*\} \\ &\approx \mathbf{f}(\infty) - \mu \left[\left(\mathbf{B}^{-1} + \beta \mathbf{h}_\nu \mathbf{h}_\nu^H\right) \mathbf{f}(\infty) - \gamma^* \sum_j a_j \frac{b_0}{\sqrt{N_0}} \mathbf{h}_\nu \right] \end{aligned} \tag{3.32}$$

which reduces to

$$\left(\mathbf{B}^{-1} + \beta \mathbf{h}_\nu \mathbf{h}_\nu^H\right) \mathbf{f}(\infty) \;\approx\; \gamma^* \sum_j a_j \frac{b_0}{\sqrt{N_0}} \mathbf{h}_\nu \tag{3.33}$$

Applying the matrix inversion lemma to (3.33), we arrive at (see Appendix B for derivation)

$$\mathbf{f}(\infty) \;\approx\; \gamma^* \frac{b_0}{\sqrt{N_0}} \frac{\sum_j a_j}{\sum_j a_j^2} \frac{1}{1+\beta\eta} \left(\sigma_t^2 \mathbf{H}\mathbf{H}^H + \sigma_w^2 \mathbf{I}\right)^{-1} \mathbf{h}_\nu \tag{3.34}$$

where

$$\eta = \frac{1}{\sum_j a_j^2} \mathbf{h}_\nu^H \left(\sigma_t^2 \mathbf{H}\mathbf{H}^H + \sigma_w^2 \mathbf{I}\right)^{-1} \mathbf{h}_\nu \tag{3.35}$$

Hence, choosing

$$\gamma = \frac{\sqrt{N_0}}{b_0^*} \frac{\sum_j a_j^2}{\sum_j a_j} (1+\beta\eta)\sigma_t^2 \tag{3.36}$$

sets $\mathbf{f}(\infty) = \mathbf{f}_{t,*}^{(\nu)}$. Fig. 3.4 shows equalizer trajectory magnitudes converging to MMSE equalizer.

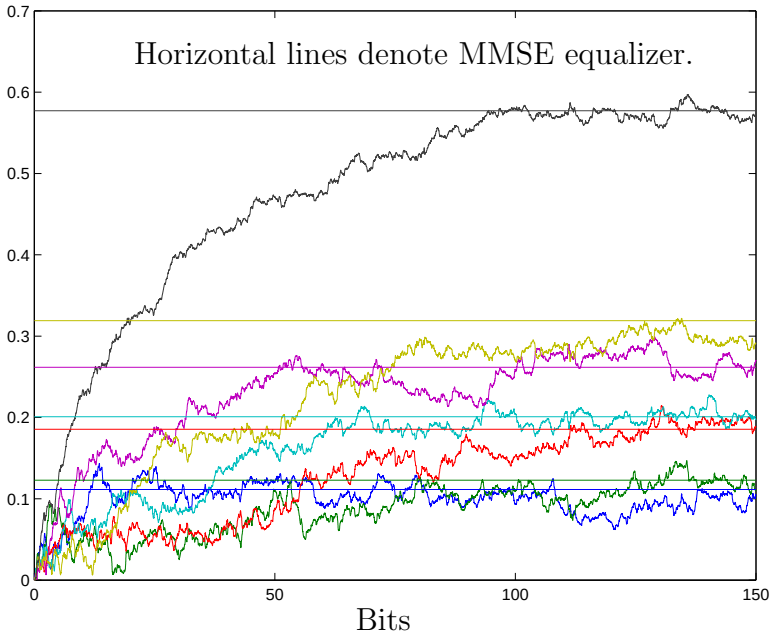

Figure 3.4: Trajectory of averaged-error LMS equalizer taps (magnitude).

CHAPTER 4

DECISION-DIRECTED EQUALIZATION

4.1 Decision-Directed Adaptation

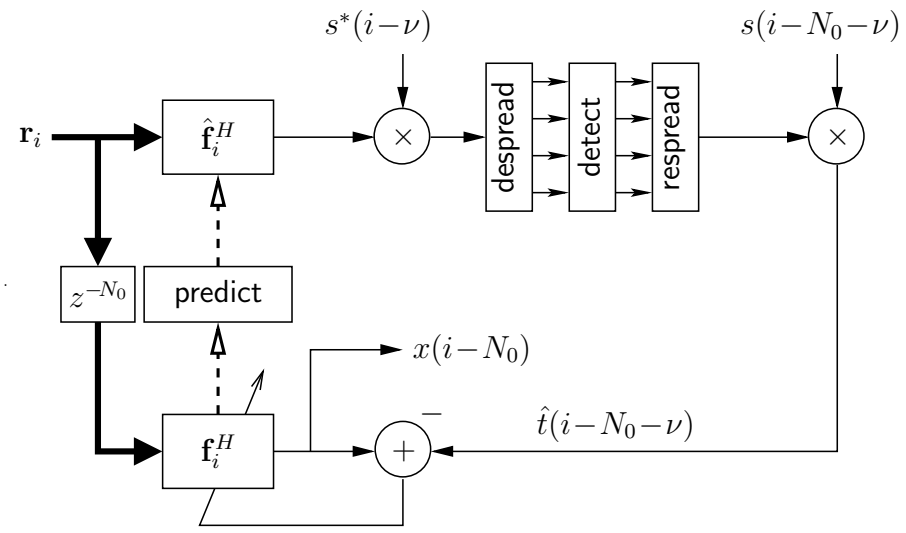

Figure 4.1: Decision directed equalization.

Assuming reasonable SNR levels, the pilot-based adaptation scheme learns and tracks the optimal equalizer reasonably well and provides an output signal from which

reliable bit decisions can be obtained. Equalizer tracking could be significantly improved, however, if we could somehow reduce the high level of MAI in the error signal.[1]

With this in mind, we propose a two-stage adaptation scheme. The first stage uses the averaged-error LMS algorithm, which is pilot trained, from Chapter 3 and is intended for "cold start-up" conditions, i.e., when the channel is completely unknown. The second stage uses bit decisions of all users (in addition to the pilot) to adapt the equalizer, as shown in Fig. 4.1. The bit decisions are obtained by despreading and detecting the output of the "tentative" equalizer $\hat{\mathbf{f}}_i$, whose values can be predicted from the decision-directed equalizer $\mathbf{f}_i$. Prediction of $\hat{\mathbf{f}}_i$ from $\mathbf{f}_i$ is necessary because $\mathbf{f}_i$ is trained on a delayed version of the received signal $\mathbf{r}_i$. Joint detection requires, in the worst case, a delay of N_0 chips, where N_0 is the spreading gain of the lowest-rate user. Arguing that, for typical mobile velocities, the equalizer taps experience relatively little change over a span of N_0 chips, the prediction can be accomplished by simply copying $\mathbf{f}_i$ to $\hat{\mathbf{f}}_i$. For best performance, final bit decisions should be made from the output $x(i - N_0)$.

The DD equalizer update equations are standard LMS

$$\begin{aligned} e(i) &= \mathbf{f}^H(i)\mathbf{r}(i-N_0) - \hat{t}(i - N_0 - \nu) \\ \mathbf{f}(i+1) &= \mathbf{f}(i) - \mu\mathbf{r}(i-N_0)e^*(i) \\ \hat{\mathbf{f}}(i+1) &= \mathbf{f}(i+1) \end{aligned} \tag{4.1}$$

Automatic adjustment of μ can be accomplished using an adaptive stepsize procedure (e.g., [55]), implying that this scheme should work well under a wide range of

[1]The main results of this chapter also appear in the manuscript [54].

conditions. The automatic step-size adjustment algorithm is

$$\begin{aligned} \mu(i+1) &= \mu(i) - \zeta \,\mathrm{Re}\{\boldsymbol{\psi}^H(i)\mathbf{r}(i-N_0)e^*(i)\} \\ \boldsymbol{\psi}(i+1) &= \left(\mathbf{I} - \mu(i)\mathbf{r}(i-N_0)\mathbf{r}^H(i-N_0)\right)\boldsymbol{\psi}(i) - \mathbf{r}(i-N_0)e^*(i) \end{aligned} \tag{4.2}$$

It should be emphasized that our decision-directed (DD) scheme is quite robust to decision errors. In the worst case–a bit error rate of 50%–the MAI power in the DD training signal $\hat{t}(i-N_0-\nu)$ will be no more than twice that of the standard LMS pilot-only training signal (assuming BPSK and equal user powers for simplicity); in the DD case, decision errors of magnitude 2 are made half the time, while in the pilot case, errors of magnitude 1 are present all the time (since we ignore the user bits altogether). Using the same reasoning, the DD algorithm will have less MAI in the error signal than the pilot only algorithm when the tentative BER is below 25%. This implies that BER=0.25 is an appropriate threshold for switching from pilot to DD.

4.2 Simulation Results

In all simulations we assume a 1/2-chip spaced, 1/2-loaded, synchronous DS-CDMA downlink consisting of one user at each of the following spreading factors: $\{4, 8, 16, 32, 64, 128, 256\}$. Users transmit with unit bit power, and the pilot power is one percent of the total transmitted power, σ_t^2. A Rayleigh-fading channel is used where the chip-spaced rays have power profile $\{0, -3, -6, -9\}$ dB and total power equal to one. Velocity is 60 km/hr, chipping rate is 3.84 Mcps, carrier frequency is 2 GHz, and the square-root raised-cosine chip waveform has excess bandwidth 0.22. The performances shown in Fig. 4.2 and Fig. 4.3 are averaged across users.

Fig. 4.2 and Fig. 4.3 show that DD adaptation significantly increases SINR and BER performance relative to pilot-only adaptation and approaches the performance of MMSE-optimal (non-adaptive) equalization. From Fig. 4.3 we note that the DD algorithm fails when SNR<0 dB. This is consistent with the reasoning in Section 4.1 since, for the first stage pilot-based algorithm, SNR<0 dB corresponds to BER>0.25. Also shown in Fig. 4.2 and Fig. 4.3 are the performances of the optimal MMSE equalizer and optimal rake receiver. Unlike the adaptive algorithms we have derived, these optimal receivers assume perfect knowledge of the time-variant channel.

Fig. 4.2 and Fig. 4.3 demonstrate that the pilot-based adaptive scheme (3.16)-(3.18) outperforms the classical adaptive rake receiver in time- and frequency-selective multipath fading. The adaptive rake receiver uses a pilot-based estimation of channel taps in which descrambled outputs were filtered using single-pole filters whose pole locations were BER-optimized through simulation.

Fig. 4.4 shows a prototypical SINR trajectory. From cold start, the pilot-based algorithm first converges to then tracks the time-varing channel. After the switch to DD, the equalizer converges closer to the optimal solution and then continues to track it.

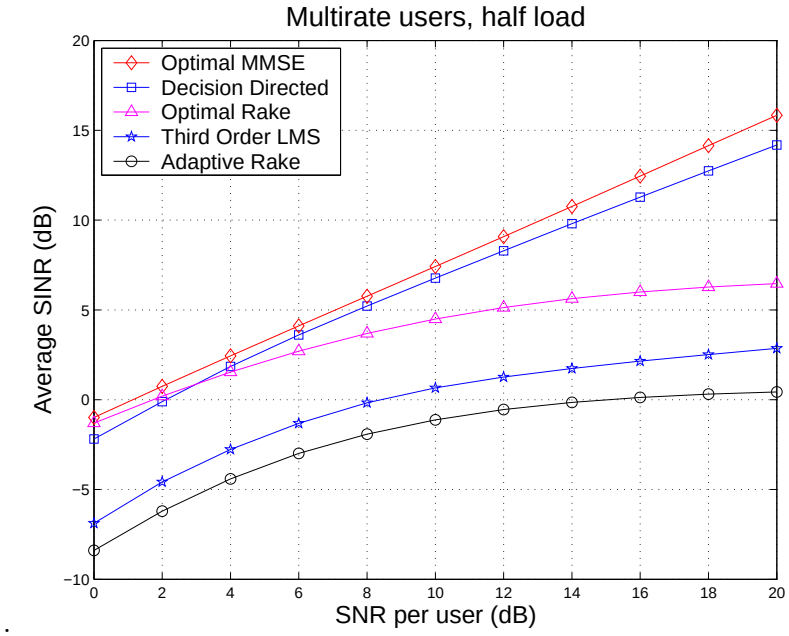

Figure 4.2: Average SINR vs SNR.

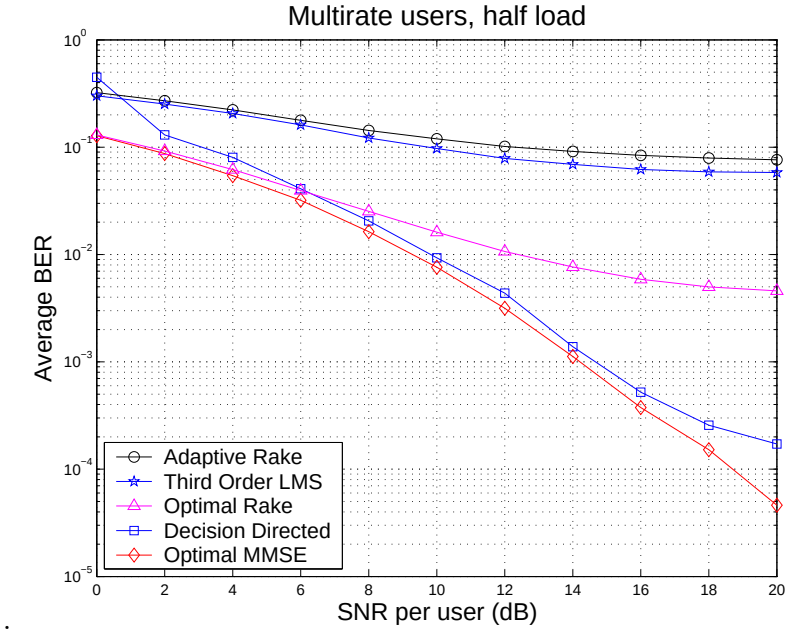

Figure 4.3: Average uncoded BER vs SNR.

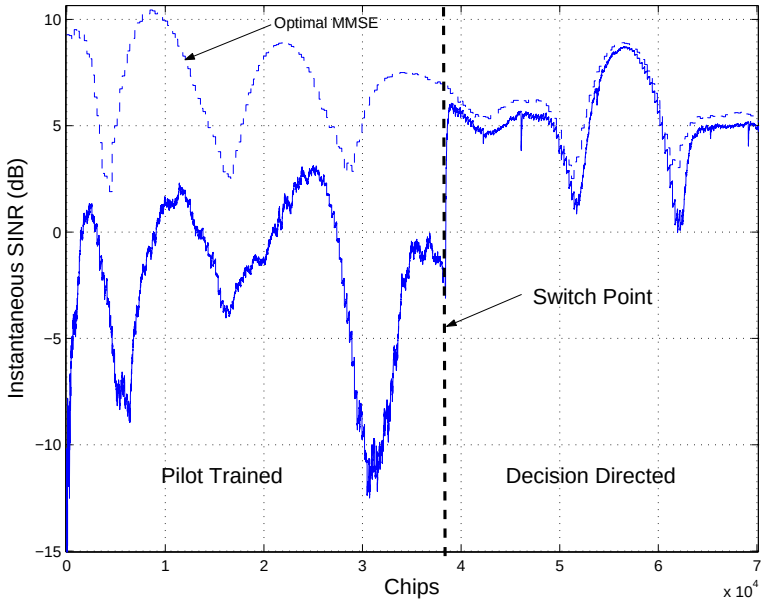

Figure 4.4: SINR trajectory form cold start to DD tracking.

CHAPTER 5

CONCLUSIONS AND FUTURE WORK

5.1 Conclusions

In this thesis we considered a downlink DS-CDMA system in which multirate user signals were transmitted via synchronous orthogonal short codes overlaid with a common scrambling sequence. Such systems are currently used in 3G cellular networks. The transmitted signal was subjected to significant time- and frequency-selective multipath fading, e.g., a channel with delay spread potentially longer than the bit interval of high-rate users.

In Chapter 3 we motivated use of a chip-rate equalizer, which restored orthogonality between the users so the de-spreading operation removed MAI in the bit estimates. We derived the optimal MMSE equalizer and determined that the pilot-trained equalizer learned the optimal. Nevertheless, there was a significant level of MAI present in the chip-rate LMS error signal. One could despread the pilot channel prior to calculating the error signal (once per bit) in order to decrease MAI; however, equalizer updates occurred less often and tracking performance suffered. We proposed recursively filtering the error signal, to provide chip-rate updates, and derived an

averaged-error LMS algorithm with enhanced tracking properties. Theoretical analysis showed that the adaptive averaged-error LMS algorithm converged to the optimal MMSE equalizer. The proposed equalizer outperformed the standard chip-rate LMS equalizer and the adaptive rake combiner.

In Chapter 4 we proposed a delayed decision-directed (DD) algorithm, which further reduced the MAI in the chip-level update, which enhanced tracking performance. The equalizer operated on the delayed received signal to allow for despread, detect, and re-spread operations. Due to the presence of the pilot signal, the DD algorithm was very robust to bit errors, and operated at a threshold of BER$<$0.25. It was shown through simulation that the performance of the DD equalizer approached the optimal MMSE equalizer.

Hence, an adaptive equalizer operated in two stages. First, a pilot-trained equalizer learned the optimal MMSE equalizer and provided reliable multiuser bit decisions. Second, bit decisions were used to reduce MAI in the error signal in a DD equalizer.

5.2 Future Work

Simulations over a wider range of channel types, mobile speeds, and spreading factors and system loads

Performance of the two-stage equalizer should be examined over a wider range of channel types and mobile speeds. In the UMTS-WCDMA specification, at least six channel types are specified over a wide range of velocities and delay spread [56]. Different spreading factors and systems loads should also be considered. A receiver must perform well under all operating conditions.

Comparison to previous work

As seen in the literature review (Section 2.5), many algorithms have been suggested. A more detailed comparison of our work with other solutions should be made.

Switch point to DD algorithm

We have suggested that the DD algorithm can operate at BER threshold of BER$<$0.25. This claim should be studied in different fading conditions to determine when to switch from the pilot-trained algorithm to DD.

Choice of μ and ρ in averaged-error LMS algorithm

We have taken for granted that the system uses optimal parameters for equalizer update. Simulations show (Fig. 3.3) that if we fix ρ we can adjust μ to provide performance near the optimal obtained by jointly optimizing both parameters. Hence, an adaptive step-size algorithm suited to the averaged-error LMS algorithm should be found.

Transient behavior

The transient behavior of the averaged-error LMS algorithm should be studied and compared to standard LMS. Overshoot and oscillations of filter parameters may be avoided by proper selection of parameters μ and ρ.

Sparse channel equalization

Simulations in this thesis have been performed on channels with relatively short delay spread. Delay spread in 3G systems may span many tens of chips. It is well known that excess mean squared error grows with the length of the equalizer; thus, sparse channel equalization algorithms, derived from our proposed methods, should be investigated.

Complexity reduction

Complexity of equalizer algorithms remains a large issue for implementation of mobile radio hand-sets. Experimentation with reduced complexity algorithms, such as signed-error signed-regressor LMS, should be done.

APPENDIX A

FADING CHANNEL SIMULATION LENGTH

In this section we answer the question: how long should a Rayleigh-fading simulation run until its results are independent of the channel realization? This is important to ask in the context of high BER simulations. Due excessive interference, the BER may be very high, which would lead to the conclusion that relatively few bits must be simulated. However, if few symbols are simulated, then the results may be too dependent on the particular channel realization over which the simulation was run. Simulations with slowly time-varying channels, i.e., channels with low doppler frequency, must be run longer than simulations with quickly varying channels. Slowly varying channels remain correlated in time much longer than quickly varying channels. Another common performance measure is the signal to interference plus noise ratio (SINR). Once again, simulations should run long enough to obtain channel realization independent results.

The correlation function of a (unit power) channel tap with Jake's spectrum is zeroth order Bessel of the first kind [5]

$$r(\tau) = J_0(2\pi f_d \tau) \tag{A.1}$$

It is easily seen in (A.1) that as the Doppler frequency f_d increases, the Bessel function compresses. The zero-mean Rayleigh-fading channel with correlation function given

by (A.1) is stationary and ergodic. The ergodicity property of the channel gives us a way to determine how long the simulation should run. Suppose a single-tap channel has unit average power, then given a desired maximum error ϵ we would like to find T' such that for $T > T'$

$$\mathrm{E}\left|\frac{1}{T}\int_0^T |h(t)|^2 \; dt - 1\right|^2 \; < \; \epsilon \tag{A.2}$$

We approximate the integral in (A.2) by discretely sampling realizations of $h(t)$, and we approximate the expectation by averaging the squared error over 10,000 channel realizations. Fig. A.1 shows a plot of MSE (defined by (A.2)) versus normalized coherence time for a single tap channel; two least-squares curve fits are also shown. We see that the MSE decreases slightly faster than inverse the simulation duration.

If we choose $\epsilon = 10^{-2}$, then from Fig. A.1 we see that the simulation must be run at least 20 normalized coherence intervals. For example, a simulation with center frequency of 2 GHz, symbol duration of 16μs, and vehicle speed of 60 km/hr (normalized coherence time is $T_{coh} = 1/(f_d T) = 562.5$) must have at least $20 \times T_{coh} = 11,250$ symbols.

It is important to note that coherence time T_{coh} is something of a misnomer. T_{coh} is defined as the inverse of the normalized maximum Doppler frequency, hence, it is the period of a sinewave. The sinewave has cycled through 360° of phase, and it is unreasonable to assume that the channel is constant over one coherence interval. A better rule of thumb is to assume the channel is fairly constant over $\frac{T_{coh}}{8}$. This is easily seen in Fig. A.2.

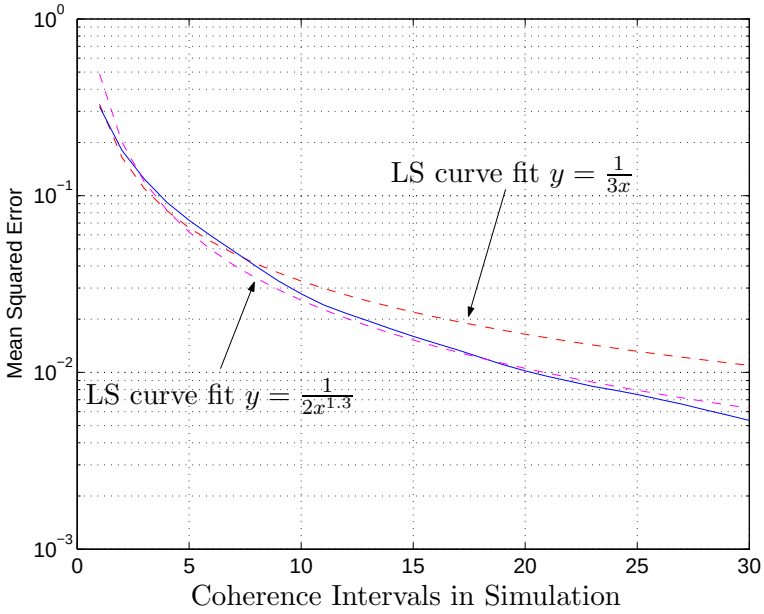

Figure A.1: MSE versus coherence time.

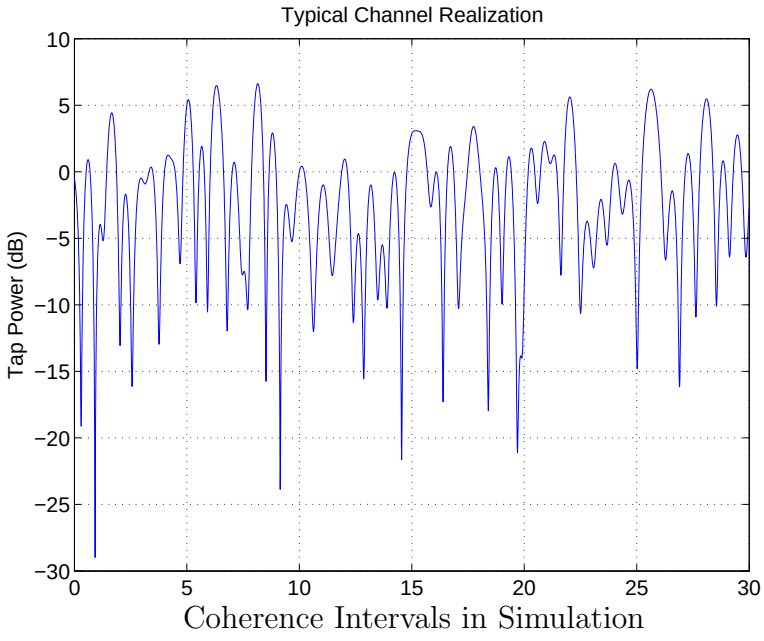

Figure A.2: Typical one-tap channel power versus normalized coherence time.

APPENDIX B

DERIVATIONS

In this appendix we derive the MMSE solutions of (3.4) and (3.6).

B.1 Derivation of Multiuser-Trained MMSE Equalizer

Recall that the cost function (3.4) is

$$J_t^{(\nu)} = \mathrm{E}\left|\mathbf{f}^H\mathbf{r}(i+\nu) - t(i)\right|^2$$

Due to A.5), the additive noise $\mathbf{w}(i)$ is white. Substituting (2.15) into (B.1) and taking the expectation using assumptions A.1), A.3), and A.5)

$$\begin{aligned} J_t^{(\nu)} &= \mathrm{E}\left|\mathbf{f}^H(\mathbf{H}\mathbf{t}(i+\nu) + \mathbf{w}(i+\nu) - t(i)\right|^2 \\ &= \mathrm{E}\left|\mathbf{f}^H\mathbf{H}\mathbf{t}(i+\nu) - t(i) + \mathbf{f}^H\mathbf{w}(i+\nu))\right|^2 \\ &= \mathbf{f}^H\mathbf{H}\Big(\mathrm{E}\left[\mathbf{t}(i+\nu)\mathbf{t}^H(i+\nu)\right] + \mathrm{E}\left[\mathbf{w}(i+\nu)\mathbf{w}^H(i+\nu)\right]\Big)\mathbf{H}^H\mathbf{f} \\ &\quad -\mathbf{f}^H\mathbf{H}\,\mathrm{E}\left[\mathbf{t}(i+\nu)t^*(i)\right] - \mathrm{E}\left[\mathbf{t}^H(i+\nu)t(i)\right]\mathbf{H}^H\mathbf{f} + \mathrm{E}\left|t(i)\right|^2 \\ &= \mathbf{f}^H\left(\sigma_t^2\mathbf{H}\mathbf{H}^H + \sigma_w^2\mathbf{I}\right)\mathbf{f} - \sigma_t^2\mathbf{f}^H\mathbf{H}\mathbf{e}_\nu - \sigma_t^2\mathbf{e}_\nu^H\mathbf{H}^H\mathbf{f} + \sigma_t^2 \end{aligned} \tag{B.1}$$

Taking the gradient of (B.1) with respect to $\mathbf{f}$ and setting to zero yields

$$\nabla_{\mathbf{f}} J_t^{(\nu)} \;=\; \left(\sigma_t^2\mathbf{H}\mathbf{H}^H + \sigma_w^2\mathbf{I}\right)\mathbf{f} - \sigma_t^2\mathbf{H}\mathbf{e}_\nu \;=\; \mathbf{0} \tag{B.2}$$

Solving (B.8) for $\mathbf{f}$, we obtain

$$\mathbf{f}_{t,*}^{(\nu)} = \sigma_t^2 \left(\sigma_t^2 \mathbf{H}\mathbf{H}^H + \sigma_w^2 \mathbf{I}\right)^\dagger \mathbf{H}\mathbf{e}_\nu \tag{B.3}$$

where $\mathbf{r}(i)$, $\mathbf{H}$, and $\mathbf{f}$ are defined in Section 2.4; $\mathbf{e}_\nu = \left[0 \ldots 0, 1, 0 \ldots 0\right]^T$, i.e., $\mathbf{e}_\nu$ is the unit vector with a one in the ν^{th} position, ($\nu \geq 0$); and $(\cdot)^\dagger$ denotes the Moore-Penrose pseudo-inverse [51].

B.2 Derivation of Pilot-Trained MMSE Equalizer

Recall the pilot-trained error function (3.6)

$$J_p^{(\nu)} = \mathrm{E}\left|s^*(i)\mathbf{f}^H\mathbf{r}(i+\nu) - \gamma\right|^2 \tag{B.4}$$

Once again, we assume that the additive noise $\mathbf{w}(i)$ is white, and we substitute (2.15) into (B.4) and take the expectation using assumptions A.1), A.3), and A.5)

$$\begin{aligned}
J_p^{(\nu)} &= \mathrm{E}\left|s^*(i)\mathbf{f}^H(\mathbf{H}\mathbf{t}(i+\nu) + \mathbf{w}(i+\nu) - \gamma\right|^2 \\
&= \mathrm{E}\left|\mathbf{f}^H\mathbf{H}\mathbf{t}(i+\nu)s^*(i) - \gamma + \mathbf{f}^H\mathbf{w}(i+\nu))\right|^2 \\
&= \mathbf{f}^H\mathbf{H}\Big(\mathrm{E}\left[\mathbf{t}(i+\nu)\mathbf{t}^H(i+\nu)\underbrace{|s(i)|^2}_{1}\right] + \mathrm{E}\left[\mathbf{w}(i+\nu)\mathbf{w}^H(i+\nu)\right]\Big)\mathbf{H}^H\mathbf{f} \\
&\quad -\gamma^*\mathbf{f}^H\mathbf{H}\,\mathrm{E}\left[\mathbf{t}(i+\nu)s^*(i)\right] - \gamma\,\mathrm{E}\left[\mathbf{t}^H(i+\nu)s(i)\right]\mathbf{H}^H\mathbf{f} + |\gamma|^2
\end{aligned} \tag{B.5}$$

Now the ℓ^{th} component of $\mathrm{E}\left[\mathbf{t}(i+\nu)s^*(i)\right]$ is

$$\begin{aligned}
\mathrm{E}\left[\mathbf{t}(i+\nu)s^*(i)\right]_\ell &= \mathrm{E}\left[t(i+\nu-\ell)s^*(i)\right] \\
&= \mathrm{E}\left[\left(\frac{b_0}{\sqrt{N_0}} + u(i+\nu-\ell)\right)s(i+\nu-\ell)s^*(i)\right] \\
&= \frac{b_0}{\sqrt{N_0}}\delta_{\nu-\ell}
\end{aligned} \tag{B.6}$$

so (B.5) can be written

$$J_p^{(\nu)} = \mathbf{f}^H\left(\sigma_t^2\mathbf{H}\mathbf{H}^H + \sigma_w^2\mathbf{I}\right)\mathbf{f} - \gamma^*\frac{b_0}{\sqrt{N_0}}\mathbf{f}^H\mathbf{H}\mathbf{e}_\nu - \gamma\frac{b_0^*}{\sqrt{N_0}}\mathbf{e}_\nu^H\mathbf{H}^H\mathbf{f} + |\gamma|^2 \tag{B.7}$$

Taking the gradient of (B.7) with respect to $\mathbf{f}$ and setting to zero yields

$$\nabla_{\mathbf{f}} J_p^{(\nu)} \;=\; \left(\sigma_t^2 \mathbf{H}\mathbf{H}^H + \sigma_w^2 \mathbf{I}\right) \mathbf{f} - \gamma^* \frac{b_0}{\sqrt{N_0}} \mathbf{H}\mathbf{e}_\nu \;=\; \mathbf{0} \tag{B.8}$$

Solving (B.8) for $\mathbf{f}$, we obtain

$$\mathbf{f}_{p,*}^{(\nu)} = \gamma^* \frac{b_0}{\sqrt{N_0}} \left(\sigma_t^2 \mathbf{H}\mathbf{H}^H + \sigma_w^2 \mathbf{I}\right)^\dagger \mathbf{H}\mathbf{e}_\nu \tag{B.9}$$

B.3 Derivation of (3.34)

Equation (3.33) states

$$\left(\mathbf{B}^{-1} + \beta \mathbf{h}_\nu \mathbf{h}_\nu^H\right) \mathbf{f}(\infty) \;\approx\; \gamma^* \sum_j a_j \frac{b_0}{\sqrt{N_0}} \mathbf{h}_\nu \tag{B.10}$$

We must find the inverse of $\left(\mathbf{B}^{-1} + \beta \mathbf{h}_\nu \mathbf{h}_\nu^H\right)$.

For $C + \mathbf{v}^H \mathbf{A} \mathbf{v} \neq 0$, the matrix inversion lemma states

$$(\mathbf{A}^{-1} + C^{-1} \mathbf{v}\mathbf{v}^H)^{-1} \;=\; \mathbf{A} - \frac{1}{C + \mathbf{v}^H \mathbf{A} \mathbf{v}} \mathbf{A}\mathbf{v}\mathbf{v}^H\mathbf{A} \tag{B.11}$$

Thus, letting $\mathbf{A} = \mathbf{B}$, $\mathbf{v} = \mathbf{h}_\nu$, $C^{-1} = \beta$, and $\eta = \mathbf{h}_\nu^H \mathbf{B} \mathbf{h}_\nu$, and using (B.11), we can write

$$\left(\mathbf{B}^{-1} + \beta \mathbf{h}_\nu \mathbf{h}_\nu^H\right)^{-1} \;=\; \mathbf{B} - \frac{1}{\frac{1}{\beta} + \eta} \mathbf{B}\mathbf{h}_\nu \mathbf{h}_\nu^H \mathbf{B} \tag{B.12}$$

hence

$$\begin{aligned}
\mathbf{f}(\infty) \;&\approx\; \gamma^* \frac{b_0}{\sqrt{N_0}} \sum_j a_j \left(1 - \frac{\eta}{\frac{1}{\beta} + \eta}\right) \mathbf{B}\mathbf{h}_\nu \\
&=\; \gamma^* \frac{b_0}{\sqrt{N_0}} \sum_j a_j \; \frac{1}{1 + \beta\eta} \mathbf{B}\mathbf{h}_\nu \\
&=\; \gamma^* \frac{b_0}{\sqrt{N_0}} \; \frac{\sum_j a_j}{\sum_j a_j^2} \; \frac{1}{1 + \beta\eta} \left(\sigma_t^2 \mathbf{H}\mathbf{H}^H + \sigma_w^2 \mathbf{I}\right)^{-1} \mathbf{h}_\nu
\end{aligned} \tag{B.13}$$

BIBLIOGRAPHY

[1] Juergen F. Roessler, Wolfgang H. Gerstacker Lutz H.-J. Lampe, and Johannes B. Huber, "Decision-feedback equalization for CDMA downlink", *Proc. IEEE Vehicular Technology Conference*, vol. 2, pp. 816–820, 2002.

[2] Michael Honig, Upamanyu Madhow, and Sergio Verdu, "Blind adaptive multiuser detection", *IEEE Trans. on Information Theory*, vol. 41, no. 4, pp. 944–960, July 1995.

[3] Ruxandra Lupas and Sergio Verdu, "Linear multiuser detectors for synchronous code-division multiple-access channels", *IEEE Trans. on Information Theory*, vol. 35, no. 1, pp. 123–135, January 1989.

[4] Gregory E. Bottomley, "Optimizing the rake receiver for the CDMA downlink", *Proc. IEEE Vehicular Technology Conference*, pp. 742–745, 1993.

[5] W.C. Jakes, *Microwave Mobile Communications*, IEEE press, Piscataway, NJ, 1993.

[6] S. Haykin, Ed., *Unsupervised Adaptive Filtering*, Wiley, New York, 1999.

[7] A. Klein, "Data detection algorithms specially designed for the downlink of CDMA systems with long spreading codes", *Proc. IEEE Vehicular Technology Conference*, pp. 203–207, May 1997.

[8] H.V. Poor, *An Introduction to Signal Detection and Estimation*, Springer, New York, NY, 2nd edition, 1994.

[9] Peter Darwood, Paul Alexander, and Ian Oppermann, "LMMSE chip equalisation for 3GPP WCDMA downlink receivers with channel coding", *Proc. IEEE Intern. Conf. on Communication*, vol. 5, pp. 1421–1425, 2001.

[10] I. Ghauri and D. T. M. Slock, "Linear receivers for the DS-CDMA downlink exploiting orthogonality of spreading sequences", *Proc. Asilomar Conf. on Signals, Systems and Computers*, pp. 650–654, November 1998.

[11] M. Lenardi and D.T.M. Slock, "A RAKE receiver with intracell interference cancellation for a DS-CDMA synchronous downlink with orthogonal codes", *Proc. IEEE Vehicular Technology Conference*, vol. 1, pp. 430–434, Spring 2000.

[12] H. Trigui, C. Fischer, and D.T.M. Slock, "Semi-blind downlink inter-cell interference cancellation for FDD DS-CDMA systems", *Proc. Asilomar Conf. on Signals, Systems and Computers*, vol. 2, pp. 1431–1435, 2000.

[13] D.T.M. Slock and I. Ghauri, "Blind maximum SINR receiver for the DS-CDMA downlink", *Proc. IEEE Internat. Conf. on Acoustics, Speech, and Signal Processing*, vol. 5, pp. 2485–2488, 2000.

[14] M. Lenardi, A. Medles, and D.T.M. Slock, "Intercell interference cancellation at a WCDMA mobile terminal by exploiting excess codes", *Proc. IEEE Vehicular Technology Conference*, vol. 3, pp. 1568–1572, Spring 2001.

[15] M. Lenardi, A. Medles, and D.T.M. Slock, "Comparison of downlink transmit diversity schemes for RAKE and SINR maximizing receivers", *Proc. IEEE Intern. Conf. on Communication*, vol. 6, pp. 1679–1683, 2001.

[16] M. Lenardi and D.T.M. Slock, "A rake structured sinr maximizing mobile receiver for the WCDMA downlink", *Proc. Asilomar Conf. on Signals, Systems and Computers*, vol. 1, pp. 410–414, 2001.

[17] S. Werner and J. Lilleberg, "Downlink channel decorrelation in CDMA systems with long codes", *Proc. IEEE Vehicular Technology Conference*, pp. 1614–1617, May 1999.

[18] M.J. Heikkila, P. Komulainen, , and J. Lilleberg, "Interference suppression in CDMA downlink through adaptive channel equalization", *Proc. IEEE Vehicular Technology Conference*, vol. 2, pp. 978–982, 1999.

[19] P. Komulainen and M.J. Heikkila, "Adaptive channel equalization based on chip separation for CDMA downlink", *Proc. IEEE Internat. Symposium on Personal, Indoor and Mobile Radio Communications*, September 1999.

[20] P. Komulainen, M.J. Heikkila, and J. Lilleberg, "Adaptive channel equalization and interference suppression for CDMA downlink", *IEEE 6th Int. Symp. on Spread-Spectrum Tech. and Appl.*, vol. 2, pp. 363–367, September 2000.

[21] M.J. Heikkila, "A novel blind adaptive algorithm for channel equalization in WCDMA downlink", *Proc. IEEE Internat. Symposium on Personal, Indoor and Mobile Radio Communications*, vol. 1, pp. A–41 –A–45, 2001.

[22] S. Werner, T. Laakso, and J. Lilleberg, "Adaptive multiple-antenna receiver for CDMA mobile reception", *Proc. IEEE Intern. Conf. on Communication*, vol. 2, pp. 1053–1057, 1998.

[23] P. Komulainen, Y. Bar-Ness, and J. Lilleberg, "Simplified bootstrap adaptive decorrelator for CDMA downlink", *Proc. IEEE Intern. Conf. on Communication*, vol. 1, pp. 380–384, 1998.

[24] C.D. Frank and E. Visotsky, "Adaptive interference suppression for direct-sequence cdma systems with long spreading codes", *Proc. Allerton Conf. on Communication, Control, and Computing*, September 1998.

[25] C. D. Frank, E. Visotsky, and U. Madhow, "Adaptive interference suppression for the downlink of a direct sequence cdma system with long spreading sequences", *special issue on Signal Processing for Wireless Communications: Algorithms, Performance, and Architecture, Journal of VLSI Signal Processing*, vol. 30, no. 1, pp. 273–291, January 2002.

[26] M. D. Zoltowski and Thomas P. Krauss, "Two-channel zero forcing equalization on CDMA forward link: Trade-offs between multi-user access interference and diversity gains", *Proc. Asilomar Conf. on Signals, Systems and Computers*, vol. 2, pp. 1541–1545, 1999.

[27] T. P. Krauss, M. D. Zoltowski, and G. Leus, "Simple MMSE equalizers for CDMA downlink to restore chip sequence: Comparison to zero-forcing and rake", *Proc. IEEE Internat. Conf. on Acoustics, Speech, and Signal Processing*, pp. 2865–2868, June 5-9 2000.

[28] G. Xu, H. Liu, L. Tong, and T. Kailath, "A least-squares approach to blind channel identification", *IEEE Trans. on Signal Processing*, pp. 2982–2993, December 1995.

[29] Thomas P. Krauss and M. D. Zoltowski, "Blind channel identification on CDMA forward link based on dual antenna receiver at hand-set and cross-relation", *Proc. Asilomar Conf. on Signals, Systems and Computers*, vol. 1, pp. 75–79, 1999.

[30] Thomas P. Krauss and M. D. Zoltowski, "Oversampling diversity versus dual antenna diversity for chip-level equalization on CDMA downlink", *Proc. IEEE Sensor Array and Multichannel Signal Processing Workshop*, pp. 47–51, 2000.

[31] Thomas P. Krauss and M. D. Zoltowski, "Chip-level MMSE equalization at the edge of the cell", *Proc. IEEE Wireless Communication and Networking Conf.*, vol. 1, pp. 386–392, September 2000.

[32] Thomas P. Krauss and M. D. Zoltowski, "MMSE equalization under conditions of soft hand-off", *IEEE Internat. Symposium on Spread Spectrum Techniques and Applications*, vol. 2, pp. 540–543, 2000.

[33] Thomas P. Krauss, William J. Hillery, and M. D. Zoltowski, "MMSE equalization for the forward link in 3G CDMA: Symbol-level versus chip-level", *Proc. IEEE Workshop on Statistical Signal and Array Processing*, pp. 18–22, August 2000.

[34] M. D. Zoltowski, William J. Hillery, and Thomas P. Krauss, "Comparative performance of three MMSE equalizers for the CDMA forward link in frequency selective multipath", *Proc. Asilomar Conf. on Signals, Systems and Computers*, vol. 1, pp. 781–785, 2000.

[35] Samina Chowdhury, M. D. Zoltowski, and J. Scott Goldstein, "Reduced-rank adaptive MMSE equalization for high-speed CDMA forward link with sparse multipath channels", *Proc. Asilomar Conf. on Signals, Systems and Computers*, vol. 2, pp. 965–969, 2000.

[36] Samina Chowdhury and M. D. Zoltowski, "Structured MMSE equalization for synchronous CDMA with sparse multipath channels", *Proc. IEEE Internat. Conf. on Acoustics, Speech, and Signal Processing*, vol. 4, pp. 2113–2116, 2001.

[37] Samina Chowdhury and M. D. Zoltowski, "Adaptive MMSE equalization for wideband CDMA forward link with time-varying frequency selective channels", *Proc. IEEE Internat. Conf. on Acoustics, Speech, and Signal Processing*, vol. 3, pp. 2605–2608, 2002.

[38] Laurence Mailaender, "CDMA downlink equalization with imperfect channel esitmation", *Proc. IEEE Vehicular Technology Conference*, vol. 3, pp. 1593–1597, 2001.

[39] Laurence Mailaender, "Low-complexity implementation of CDMA downlink equalization", *Internat. Conf. on 3G Mobile Communication Technologies*, pp. 396–400, 2001.

[40] Kemin Li and Hui Liu, "A new blind receiver for downlink DS-CDMA communications", *IEEE Communications Letters*, vol. 3, no. 7, pp. 193–195, July 1999.

[41] Frederik Petre, Marc Moonen, Marc Engels, Bert Gyselinckx, and Hugo De Man, "Pilot-aided adaptive chip equalizer receiver for interference suppression in DS-CDMA forward link", *Proc. IEEE Vehicular Technology Conference*, vol. 1, pp. 303–308, September 2000.

[42] Frederik Petre, Geert Leus, Marc Engels, Marc Moonen, and Hugo De Man, "Semi-blind space-time chip equalizer receivers for WCDMA forward link with code-multiplexed pilot", *Proc. IEEE Internat. Conf. on Acoustics, Speech, and Signal Processing*, vol. 4, pp. 2245–2248, May 2001.

[43] Frederik Petre, Geert Leus, Luc Deneire, Marc Engels, Marc Moonen, and Hugo De Man, "Space-time chip equalizer receivers for WCDMA forward link with time-multiplexed pilot", *Proc. IEEE Vehicular Technology Conference*, vol. 2, pp. 1058–1062, October 2001.

[44] Frederik Petre, Geert Leus, Luc Deneire, Marc Engels, and Marc Moonen, "Space-time chip equalizer receivers for WCDMA downlink with code-multiplexed pilot and soft handover", *Proc. IEEE Global Telecommunications Conf.*, vol. 1, pp. 280–284, 2001.

[45] Frederik Petre, Geert Leus, Luc Deneire, Marc Engels, and Marc Moonen, "Adaptive space-time chip-level equalization for WCDMA downlink with code-multiplexed pilot and soft handover", *Proc. IEEE Intern. Conf. on Communication*, vol. 3, pp. 1635–1639, April 2002.

[46] Geert Leus, Frederik Petre, and Marc Moonen, "Space-time chip equalization for space-time coded downlink CDMA", *Proc. IEEE Intern. Conf. on Communication*, vol. 1, pp. 568–572, April 2002.

[47] Gregory E. Bottomley, Tony Ottosson, and Yi-Pin Eric Wang, "A generalized RAKE receiver for interference suppression", *IEEE Journal on Selected Areas In Communications*, vol. 18, no. 8, pp. 2333–2339, August 2000.

[48] Yi-Pin Eric Wang and Gregory E. Bottomley, "Generalized RAKE reception for cancelling interference from mulitple base stations", *Proc. IEEE Vehicular Technology Conference*, pp. 2333–2339, 2000.

[49] Monish Ghosh, "Adaptive chip-equalizers for synchronous DS-CDMA systems with pilot sequences", *Proc. IEEE Global Telecommunications Conf.*, vol. 6, pp. 3385–3389, 2001.

[50] Jingnong Yang and Ye (Geoffrey) Li, "A decision-feedback equalizer with tentative chip feedback for the downlink of wideband CDMA", *Proc. IEEE Intern. Conf. on Communication*, vol. 1, pp. 119–123, 2002.

[51] G. Strang, *Linear Algebra and its Applications*, Harcourt Brace Jovanovich, Fort Worth, TX, 3rd edition, 1988.

[52] W. A. Sethares, B. D. O. Anderson, and C. R. Johnson, "Adaptive algorithms with filtered regressor and filtered error", *Mathematics of Control, Signals, and Systems*, vol. 2, pp. 381–403, July 1989.

[53] S. Gazor, "Prediction in lms-type adaptive algorithms for smoothly time varing environments", *IEEE Trans. on Signal Processing*, vol. 47, pp. 1735–1739, June 1999.

[54] Phil Schniter and Adam Margetts, "Adaptive chip-rate equalization of downlink multirate wideband CDMA", *Proc. Asilomar Conf. on Signals, Systems and Computers*, November 2002.

[55] A. Benveniste, M. M'etivier, and P. Priouret, *Adaptive Algorithms and Stochastic Approximations*, Springer-Verlag, Paris, France, 1990.

[56] *Third Generation Partnership Project, TS GRAN 25.943*, 2002.